12-5-2008

Surface Water and Ground Water Interactions of the Rio de las Vacas, NM; Characterizing Exchange and Predicting Response Using Thermal Data

Andrew Robertson

Surface Water and Ground Water Interactions of the Rio de las Vacas, NM; Characterizing Exchange and Predicting Response Using Thermal Data

A Professional Project Report Submitted in Partial Fulfillment of the Requirements for the Degree of
Master of Water Resources:
Hydroscience Concentration

Andrew Robertson

Water Resources Program
The University of New Mexico
Albuquerque, New Mexico
December 2008

Contents

Figures

Tables

Acknowledgements

I would like to thank the Graduate and Professional Student Association (GPSA), the Student Research Allocations Committee (SRAC), and the Office of Graduate Studies (OGS) for funding this work. I would also like to thank Global Water Instrumentation, Inc. and Rodgers & Company, Inc., especially Jeff Watson and Mike Lucero, for discounted products and expert advice. I would like to acknowledge Julie Watson and Nina Wells at the New Mexico Environment Department and Mike Dechter of the U.S. Forest Service for supporting this project, and my colleagues at the New Mexico USGS Water Science Center for their advice and encouragement. I would also like to acknowledge those individuals who were directly involved in the field work, analysis and editing including James Robertson, Monique Robertson, Keith Laffler and Kurt McCoy. Finally, thanks to my committee members Dr. Julie Coonrod, Dr. Cliff Dahm, and Dr. Bruce Thomson and to Annamarie Cordova for seeing this project through and acting in a timely manner to ensure my success.

I. Abstract

Temperature signatures in the hyporheic zone of a perennial, northern New Mexico stream suggest a complex and dynamic system of interactions on a diurnal time scale. Fourteen shallow wells were instrumented with temperature data loggers and installed along four transects across a 40 ft reach of a proposed, channel-modifying restoration structure on the Rio de las Vacas. Temperature signatures in the banks and the floodplain of the reach suggest a parallel flow system while the instream wells suggest a losing reach within 15 to 30 in. of the stream bed. The thermal signatures of a losing reach that appear at the shallow depths dissipate at greater depths below the stream. Hydraulic head measurements alone, do not adequately describe the subsurface dynamics. This study suggests that the subsurface flow regime includes discrete flow paths that have minimal interaction and their discharge characteristics are temperature dependant. As a result of the temperature data, the overall estimated ground water exchange currently decreases from 0.43 cubic feet per second (cfs) to 0.40 cfs at bankfull and 0.21 cfs to 0.20 cfs at baseflow. The estimated increase in exchange from adding 7 feet of stream length with the proposed structure decreases from 0.49 cfs to 0.45 cfs at bankfull and 0.24 cfs to 0.23 cfs at baseflow conditions. The restricted loss of stream water to the subsurface reduces the residence time in the subsurface. Therefore gains in thermal stability by adding surface area over which the exchange could occur, would likely not counter the increase in stream temperatures from increased exposure to solar radiation.

II. Introduction

Objectives

Data were collected from June 2007 to July 2008 to characterize the surface water and ground water exchange characteristics in a 40 foot reach of the Rio de las Vacas. The objectives of this study were to: (1) characterize the surface water and ground water exchange prior to the installation of channel-modifying structures, (2) compare the predicted response of hydraulic data to thermal data, (3) predict the impacts on this exchange with a change in channel morphology and (4) make reasonable assumptions of the flow regime controls.

Significance

Society benefits from the ecological services provided by functionally intact and biologically complex freshwater ecosystems. Such services include: provisions (e.g. products, drinking water and food), supports (e.g. waste processing and nutrient cycling), and enriching or cultural services (e.g. aesthetics and recreation) (Giller, 2005). These services are increasingly compromised as freshwater habitats and organisms have become threatened (Palmer et al., 2005). Indeed, species loss is greater in freshwater habitats than in any other ecosystem (compared to terrestrial and marine habitats) (Jenkins, 2003). In New Mexico, the state environment department in compliance with Section 303(d)(1) of the Clean Water Act, reports that “[f]rom a total of over 6,561 primarily perennial stream

miles, almost 2,612 assessed miles, or 40%, have identified impaired designated or attainable uses..." (NMWQC, 2006).[1]

Thus, there is a recognized need to restore and maintain rivers and streams for the current and future services they provide. "River restoration projects aim to increase ecosystem goods and services, and ideally convert damaged freshwater systems into sustainable ones whilst protecting downstream and coastal ecosystems." (Giller, 2005).

One important component of freshwater ecosystems is the benthos and hyporheic zones. "…understanding how water within the fluvially derived sediments and the stream channel interacts is critical to efforts attempting to protect both ground water and surface water resources, and the stream and riparian ecology" (Woessner, 2000). Of late, interactions and functions of the near channel sediments have received considerable attention from the research community. However, there has been little attempt to incorporate this research into restoration models or in post-assessment of completed projects.

This study was originally begun as an effort to employ additional hyporheic monitoring to a specific, channel-modifying structure as part of a federally funded restoration project[2], thus enhancing the success of the project by providing added benefits, including

[1] The document also reports the total size of impairment due to thermal effects is 1,054 miles (16.1%) and sedimentation/siltation as 1,015 miles (15.5%) (out of 6,561 stream miles).
[2] "Rio de Las Vacas Wetlands Restoration Project" funded under the FY05 EPA Wetlands Program Development Grant Program, Region 6 CWA Section 104(b)(3).

scientific contribution and improved methods without any lasting harm, included as attributes of a successful restoration project outlined by Palmer et al. (2005).

The scientific contribution this project may have on the overall Rio de las Vacas Restoration Project is to predict the hyporheic response to induced morphological changes in the stream channel. As noted above, little work has been done, to link the groundwater response to restoration projects and to channel meanders. The value of thermal monitoring methods may benefit research on stream/groundwater interactions that are becoming increasingly inseparable to freshwater ecological research and thus restoration work.

As noted in several studies, it is critical to the understanding of the shallow alluvial flow paths for near continuous data collection to determine small temporal variations. "Understanding of the stream-groundwater system interactions requires knowledge of subsurface flow pathways and their linkage with streams, rates of flow within and between these two domains, and variation in these processes both spatially (transect, reach, watershed) and temporally (diel, seasonal, and annual)." **(**Wroblicky et al., 1992).

Exchange between the surface and ground water provides an indication of the value of stream bank storage, flood attenuation, nutrient exchange, temperature stability and added hyporheic biota. These factors are instrumental in determining the immediate system's ecology including cold water species habitat, water quality and species diversity, as well as downstream implications.

Previous Work

Near Channel Ground Water Exchange

Previous work has determined that there are many elements involved in producing surface and shallow ground water exchanges. Spatial and temporal elements combine in a series of variables to produce a dynamic system that provides stability and resilience to the stream/river system. Potential differences can result from geologic elements, including variation in sediment features (e.g. porosity) (Vaux, 1962), positive relief features (Jobson and Carey 1989, Savant et al., 1987) and overall topography (Harvey and Bencala, 1993). The direction and magnitude of vertical hydrologic exchange within headwater streams has been shown to be dependant upon not only the geologic setting but also the stream discharge (Henry et al., 1994).

Stream discharge is the manifestation of climatic elements, and watershed characteristics (especially size), that along with flooding and drought, influence interactions on an annual, seasonal, and diurnal time scale (Harvey and Bencala, 1993, Lee and Hynes, 1977, Triska et al., 1990, Valett, 1993). Henry et al. (1994) also reported that diurnal fluctuations in the hydraulic head corresponded to evapotranspiration rates suggesting a strong connection between the hyporheic and riparian zones.

Research on the hyporheic zone has offered insight into the functional significance and enormous ecological importance of stream and shallow aquifer exchange. Studies have been performed on nutrient cycling (Dahm et al., 1998, Grimm and Fisher, 1984) of

carbon (Dahm et al,. 1991, Hemond, 1990), nitrogen (Duff and Triska ,1990, Hill, 1990, Lowrance et al., 1984, Peterjohn and Correll, 1984, Triska et al., 1989, Triska et al., 1990) and dissolved oxygen (Woods, 1980) and solute transport (Harvey and Bencala 1993), and have identified benthos specific flora and fauna (Boulton et al., 1992, Coleman and Hynes, 1970, Danielopol, 1989) and the impacts on microbial dynamics (Hendricks, 1993) and overall stream metabolism (Dahm et al., 1991, Grimm and Fisher, 1984)

Research has suggested that groundwater interaction plays a role in algal and macrophyte abundance (Coleman and Dahm, 1990, Fortner and White, 1988, Hendricks and White, 1988), which directly determine the streams ability for primary production. Numerous investigators have demonstrated the importance of the stream channel exchange on fish habitat (Baxter and Hauer, 2000, Benson, 1953, Cunjak and Power, 1986, Curry and Noakes, 1995, Ebersole et al., 2001, Garrett et al., 1998, Hansen, 1975, Nielson et al., 1994, Sowden and Power, 1985, Vaux, 1962) and there is growing evidence that the hyporheic zone may play a significant role in riparian vegetation (Kondolf et al., 1987, Triska et al., 1993, Henry et al., 1994, Valett, 1993)

Most studies to date on near-channel, ground and surface water interactions have been done using piezometers to measure the hydraulic potential differences in near-channel sediments and the surface water (Baxter and Hauer, 2003, Henry et al., 1994, Dahm and Valett, 1996, Geist, et al., 1998, Stanford et al., 1994, Wroblicky et al., 1992). Other techniques include winter ice observations (Baxter and Hauer, 2000, Benson, 1953), dye

and tracer experiments (Dahm and Valett, 1996, Harvey and Bencala, 1993, Triska et al., 1989) and accretion studies of stream flow (Kondolf et al., 1987, Riggs, 1985, Stanford et al., 1994).

Temperature Studies

Using temperature in groundwater studies began with Keys and Brown (1978) using temperature as a tracer to map groundwater movement. Silliman and Booth (1993) used temperature to identify gaining, neutral or losing reaches in streams and two years later performed and presented a qualitative method for estimating water flux through stream sediments based upon temperature time series (Silliman et al., 1995). Ebersole et al., 2001 mapped the stream bed temperatures of streams and suggested that cool upwelling ground water may allow some refugia for rainbow trout in warm stream reaches. More recently Torgersen et al., (2001) used airborne thermal remote sensing to determine groundwater inflows. For a review of the use of temperature in ground water studies see Anderson (2005).

Conceptual Description

Three flow regimes are possible when considering ground water / surface water interactions:

- Gaining reach – temperature driven by advection in ground water; little variation in time
- Zero Flux – temperature driven by conduction with no mass exchange.

- Losing reach – sediment temperatures should reflect surface temperatures with a lag in phase resulting from travel time and reduced amplitude, advective driven process

Background

Study Location

The Rio de las Vacas (HUC code 130202020201) is located in north-central New Mexico (Figure 1). The head waters are in Rio Arriba County and flow through Sandoval County. The Rio de las Vacas watershed is approximately 101,343 acres and is 25.1 miles long. It is a part of the Jemez River watershed and the larger Rio Grande Basin. The Rio de las Vacas is a perennial, 5^{th} order stream with headwaters originating from springs in the San Pedro Parks Wilderness (Ferrell et al. 2003).

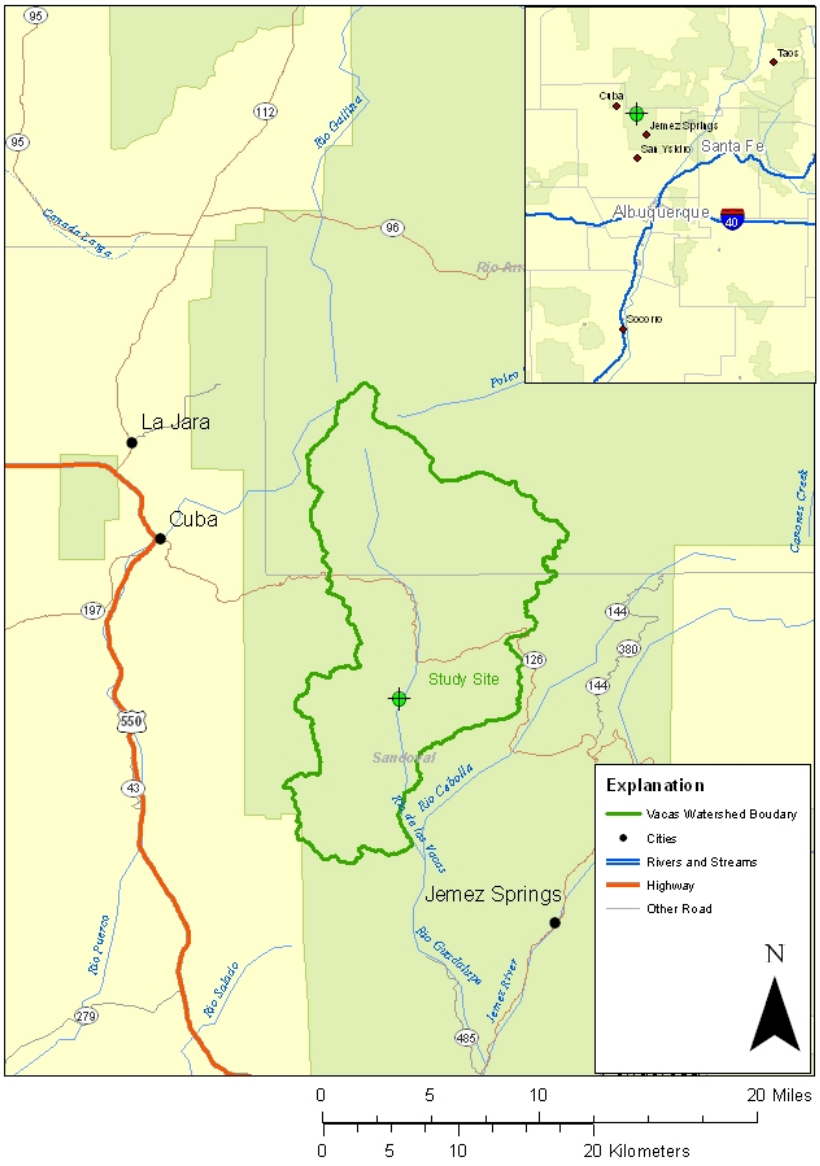

Figure 1. Map of study site location.

The valley is composed of Bandelier Tuff to the east and Precambrian Granite to the west. The alluvial valley fill overlays Abo and Madera limestones.

Vegetation

The site is located at approximately 7,900 feet above mean sea level and surrounding hillslopes host mixed conifers. The valley bottom is mostly open and covered with grasses and wetland species such as cattails and sedges in low lying areas. Alders and dogwoods are sparse but present upstream and downstream of the site (Figure 2).

Figure 2. Photo viewing upstream (north) from transect 3 prior to well emplacement.

Channel Description

The study reach drains approximately 63,389 acres (99 sq. mi.) The reach is characterized by a long straight run, terminating in a pool. The left bank includes a 4 foot cutbank

(Figure 2) into a small terrace and steeply rising hill slope interrupted by the road cut. The right bank slopes gradually out of the stream (Figure 3).

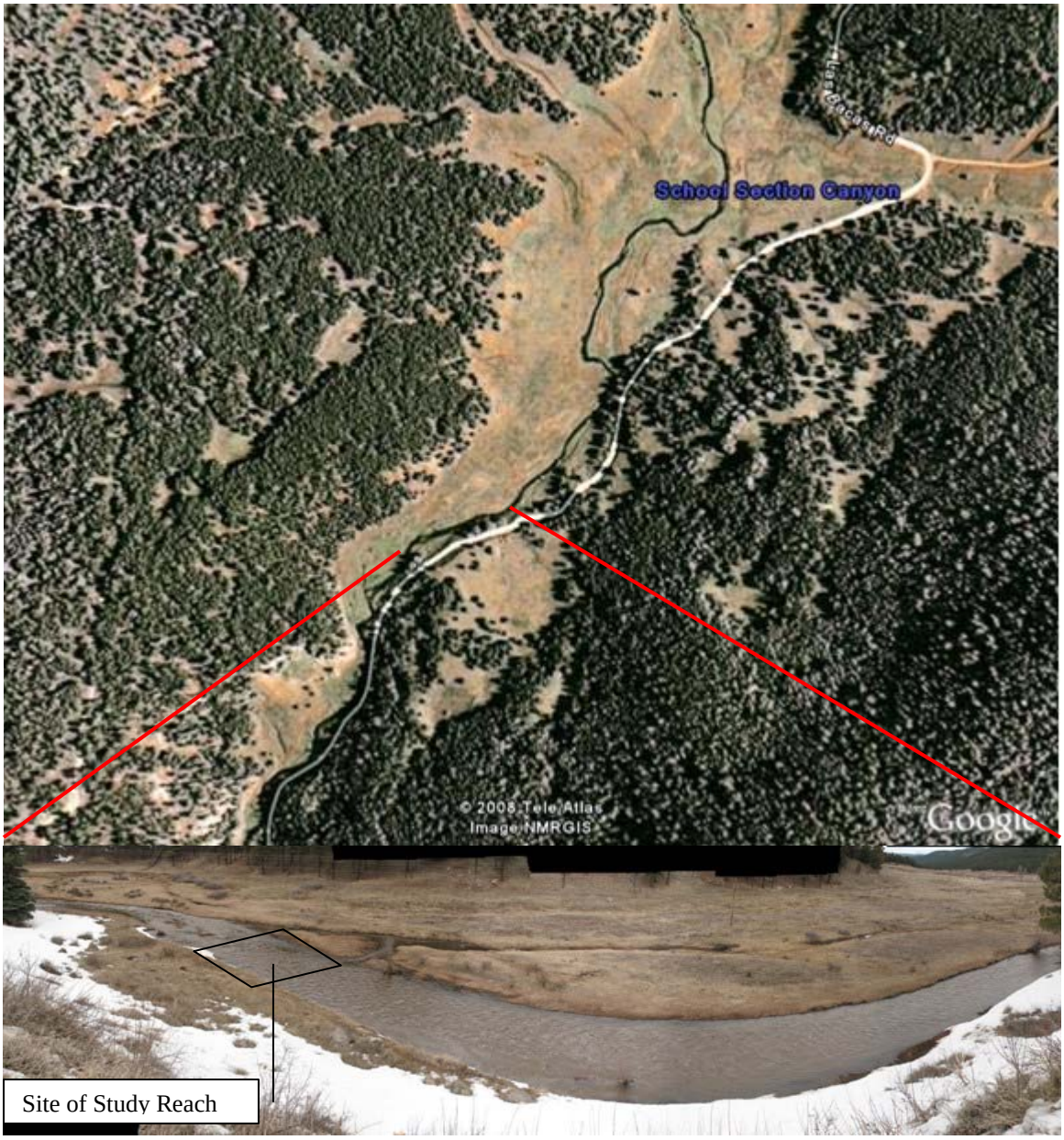

Figure 3. Aerial photo of study site and photo looking over stream from hill to river left.

An abandoned channel is located almost midway through the floodplain (Figures 3 and 4) and is perennially wet and flows in large runoff events. Surveyed flood debris in the summer of 2007 shows a stream stage that would have submerged the high ground between the main channel and the abandoned channel.

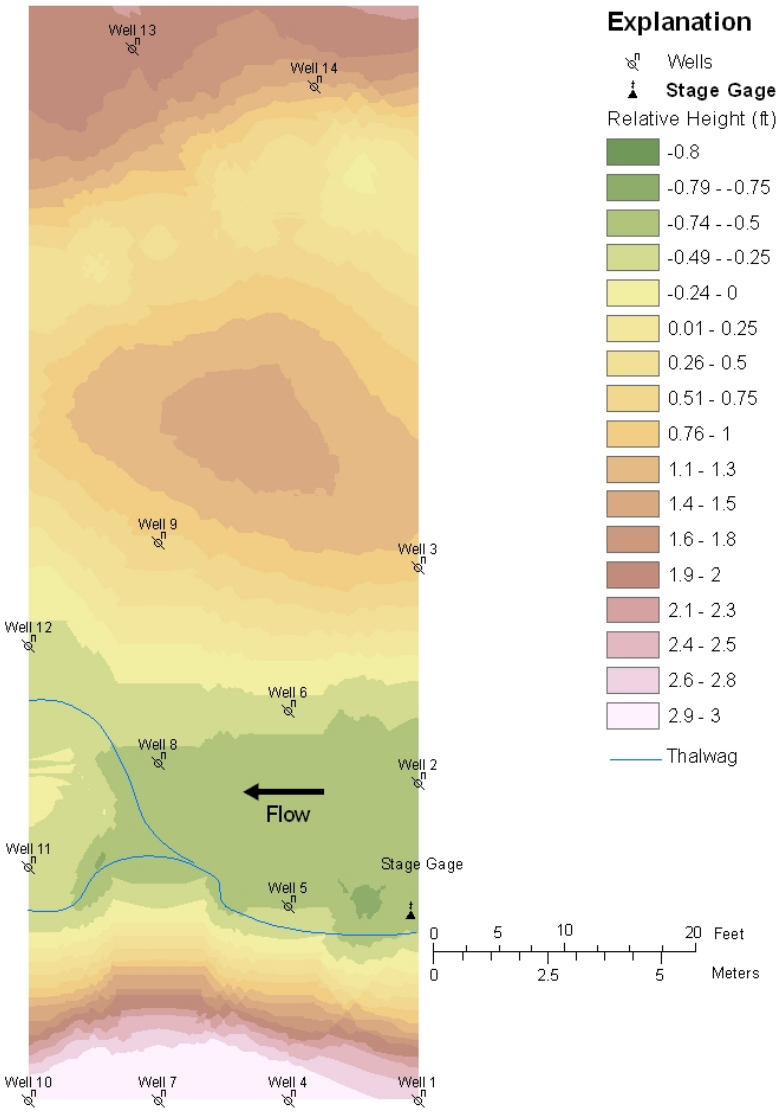

Figure 4. Plan view of study site, bottom of figure is the left bank and stream flow is right to left. Relative land surface elevations are Kriged data from cross-sectional surveys.

Above bankfull, water is capable of accessing the abandoned channel 50 feet from the cut bank (Figure 5). The average bankfull dimensions calculated for each transect are given in Table 1. The bankfull dimensions were calculated using a roughness coefficient (Manning's *n*) of 0.040.

	Average	Standard Deviation
Bankfull Dimensions		
Cross-sectional area (ft.sq.)	55	11
Width (ft)	52	12
Mean depth (ft)	1.1	0.1
Maximum depth (ft)	2.0	0.1
Hydraulic radius (ft)	1.1	0.1
Width-depth ratio	49	14
Bankfull Flow		
Velocity (ft/s)	2.1	0.1
Discharge rate (cfs)	116	22
Froude number	0.36	0.01
Flood Dimensions		
Width of flood prone area (ft)	91	8
Entrenchment ratio	1.9	0.5

Table 1. Bankfull stream dimensions; (ft. sq. = square feet, ft = feet, ft/s = feet per second, cfs = cubic feet per second)

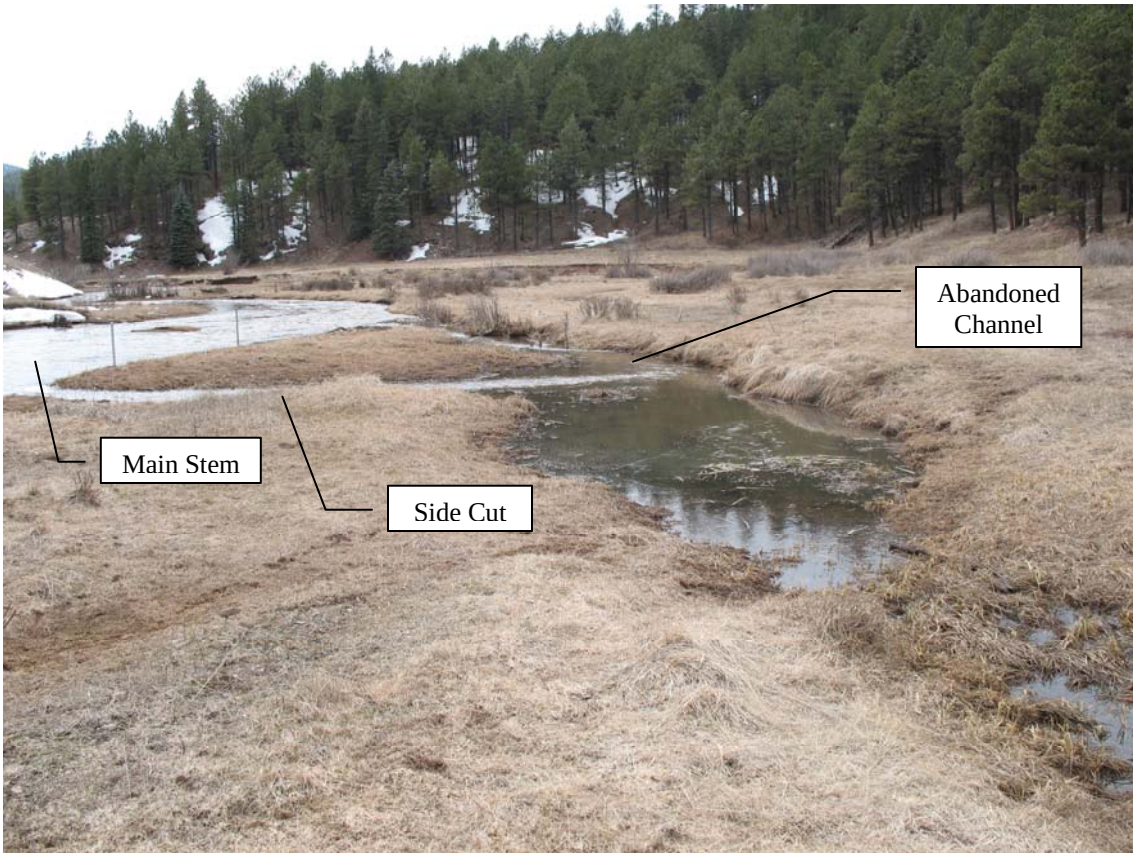

Figure 5: Photo looking downstream from right bank. The side cut entering from the main stem to the left is flowing water. Water upstream of the side cut is still from back water and ground water.

The thalwag within the reach becomes less well defined as the stream flows from the top to the bottom of the reach. The longitudinal profile (Figure 6) shows a slight increase in the bed depth from the top of the reach to just before entering the downstream pool.

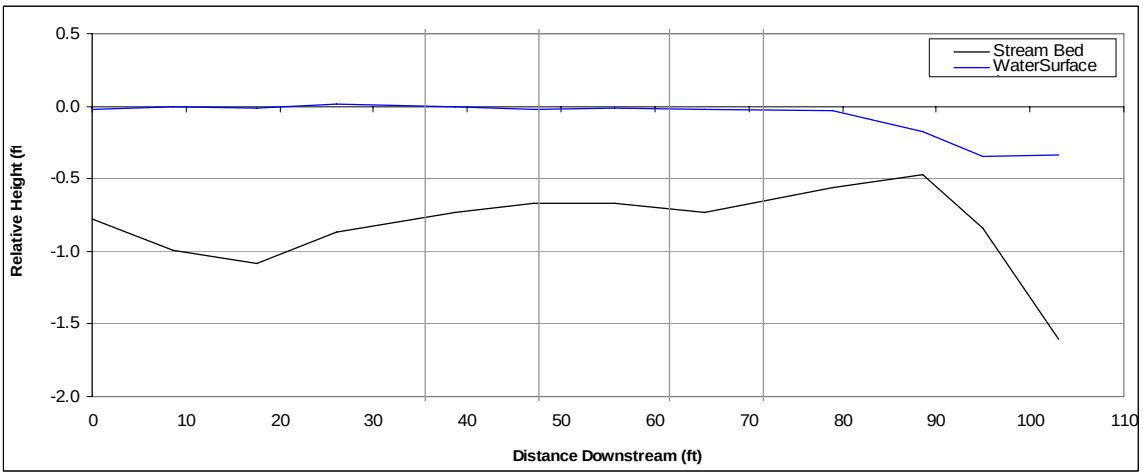

Figure 6. Longitudinal profile of reach. Stream flow is left to right. Vertical lines represent transect positions 1 to 4, from left to right.

The Wolman pebble count (Wolman, 1954) technique was performed to determine the size of clasts within the reach. From the 93 samples taken the bed material was determined to be 20% sand, 52% gravel, 26% cobble and 2% boulder. There was also a noticeable film of silt/clay on the bedding when surveyed in June 2007. The D50 grain size is 1.46 in (37 mm). The exposed surface of the cut bank appears to be composed of mainly clays and fines, while the flood plain shows mainly larger clasts both sorted and unsorted and clear examples of imbrication suggesting a continually moving channel.

Climate

The climate for the study site is typical of a high elevation, semi-arid zone. Average summer temperatures are around 60° F and teens for the winter. There were significant monsoon events in August and September and snow accumulations in December through

February or March. Figure 7 displays the daily maximum, minimum and average temperatures collected at the site.

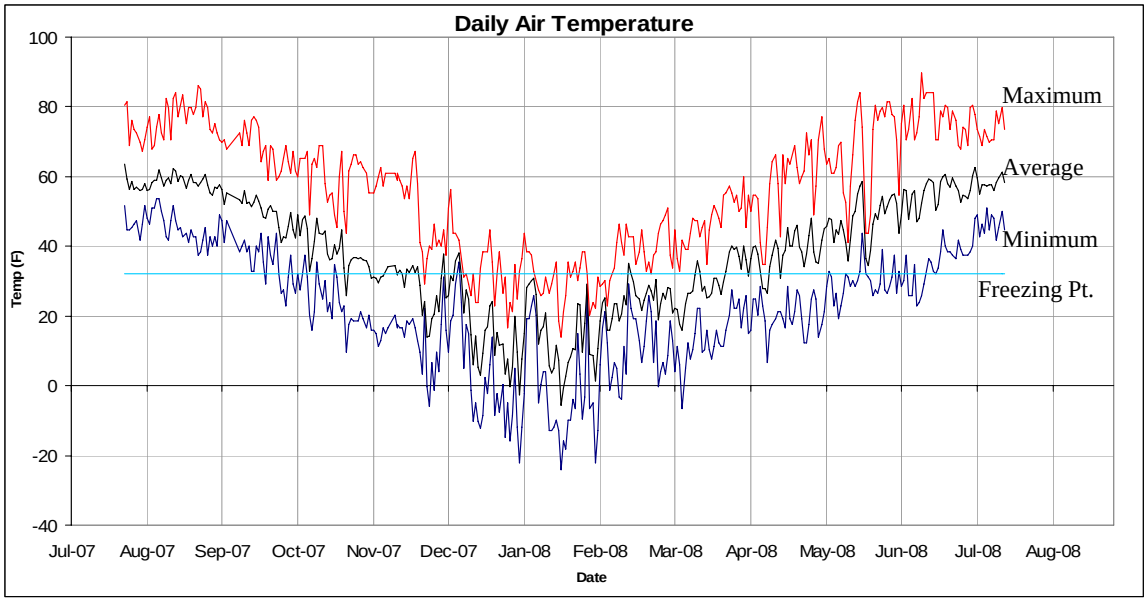

Figure 7. Daily temperature statistics measured at the study site.

III. Methodology

Site Selection

As described above, the water body was chosen to accompany a federally-funded restoration project. The specific reach was chosen for access, limited traffic, downstream location, planned structure type and topography.

Well Construction

Wells were constructed using 5 and 3 foot sections of 1 ½ inch galvanized steel pipe and installed on June 24 and 25, 2007. The length of the well was adjusted by using various sections and fastened together with steel couplings. Each well included a wire-wrapped steel drive point, and end cap.

To place the wells in the ground, a hole was started by pounding a steel “rock-breaking” rod into the ground. After the hole was started the drive point and risers of appropriate length were driven in using a slide hammer and/or sledge hammer. The screened sections were completed at various depths targeting the top of the screen ½ to 1 foot below the water table in the wells on banks and floodplain and ½ to 1 foot below the streambed for instream wells. Figure 8 shows a comparison of the well constructions including top of casing (TOC) and screened sections.

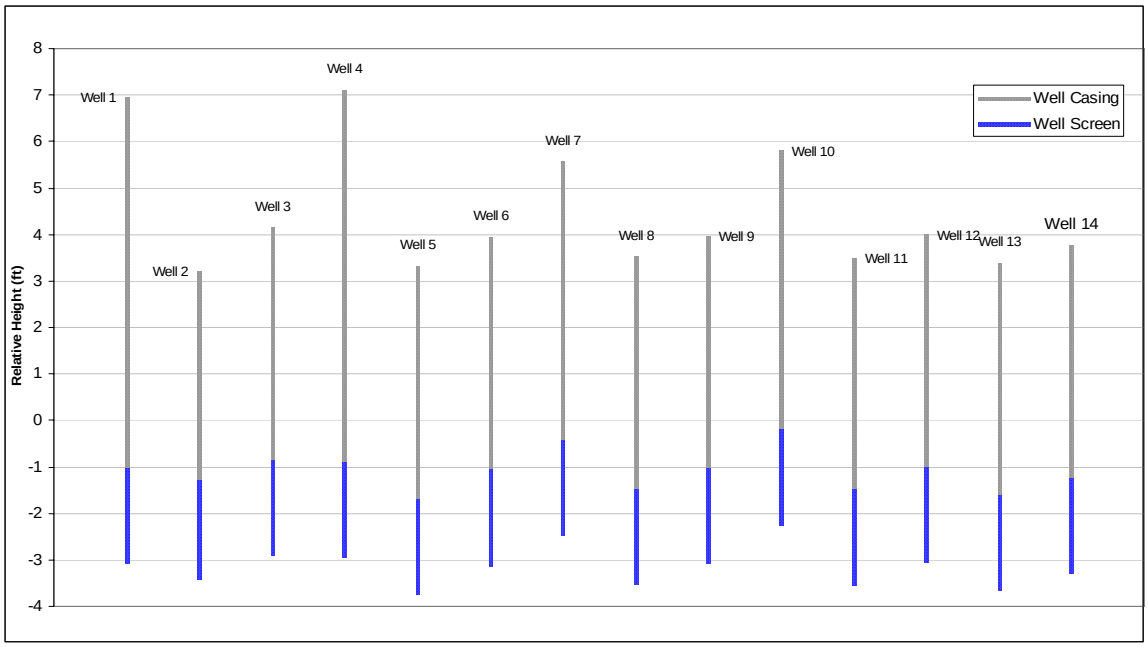

Figure 8. All wells and their relative TOC and screened interval heights. (0 feet is an arbitrary stream base flow height on June 24, 2007.)

The wells were installed along four transects that crossed the stream from the left to the right bank. The transects were established by creating the upstream transect 10 feet above the top of the planned structure and then at 10 foot intervals downstream. Each transect includes 3 wells, one well on the left bank and the remaining two staggered as to capture a smaller horizontal gap (Figure 9). Finally 2 wells were installed in the flood plain far to the right and across from an abandoned channel.

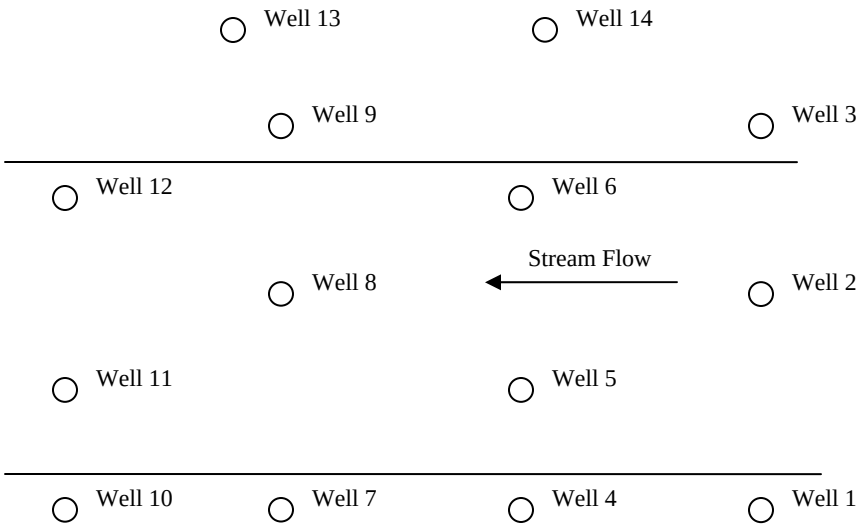

Figure 9. Conceptual plan view of well placement in reach.

Figure 10, 11, 12 and 13 represent transects 1, 2, 3 and 4 respectively. Transect 1 is the upstream transect and transect 4 is the downstream transect.

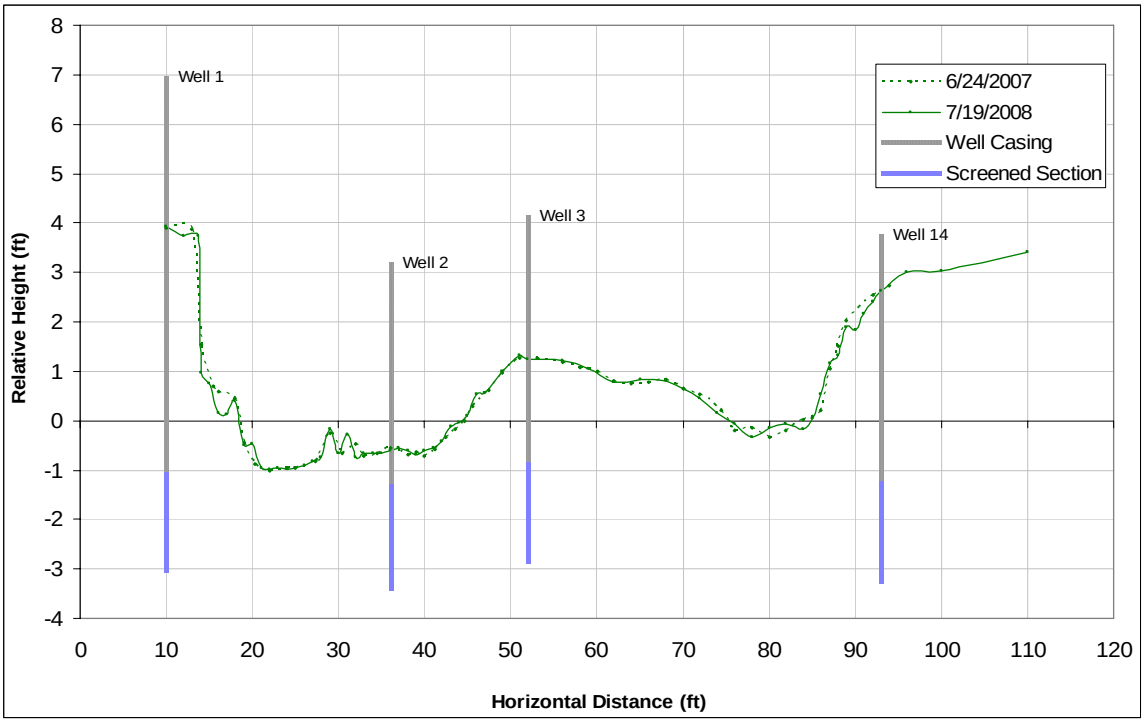

Figure 10. Well locations on transect 1, the most upstream transect. Green lines are surveyed cross-section dimensions at post-run off flows for 2007 and 2008. Base flow on 6/24/07 is 0 ft reference.

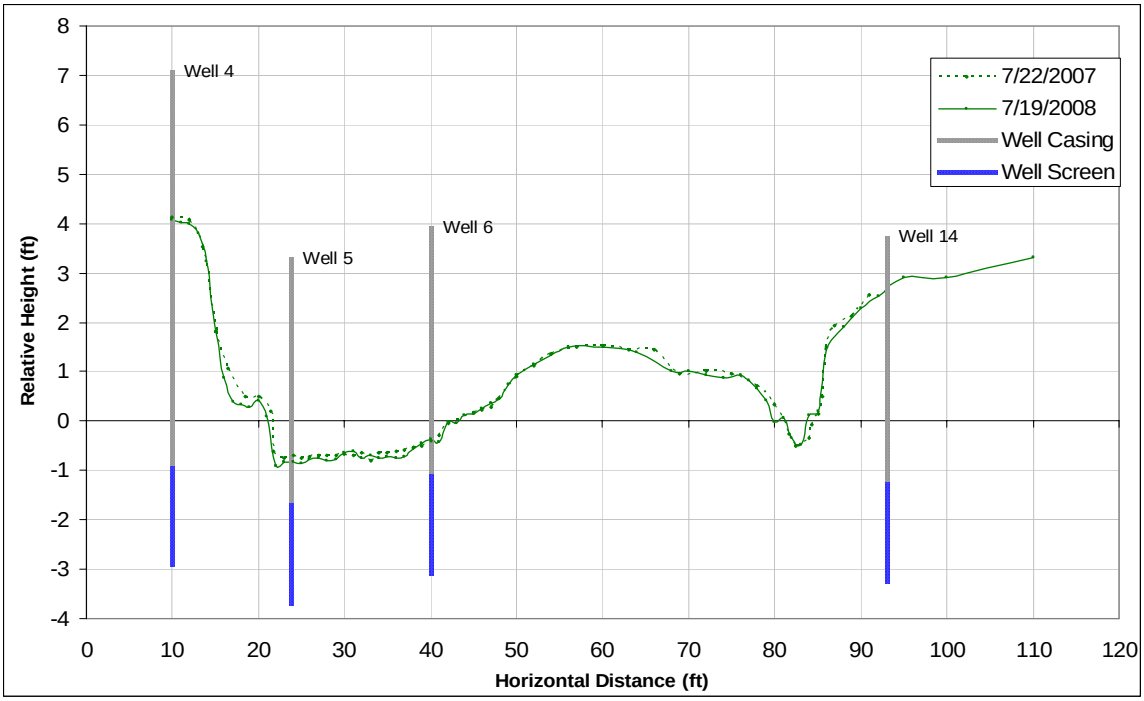

Figure 11. Well locations on transect 2; 10 feet downstream of transect 1. Green lines are surveyed cross-section dimensions at post-run off flows for 2007 and 2008. Base flow on 6/24/07 is 0 ft reference.

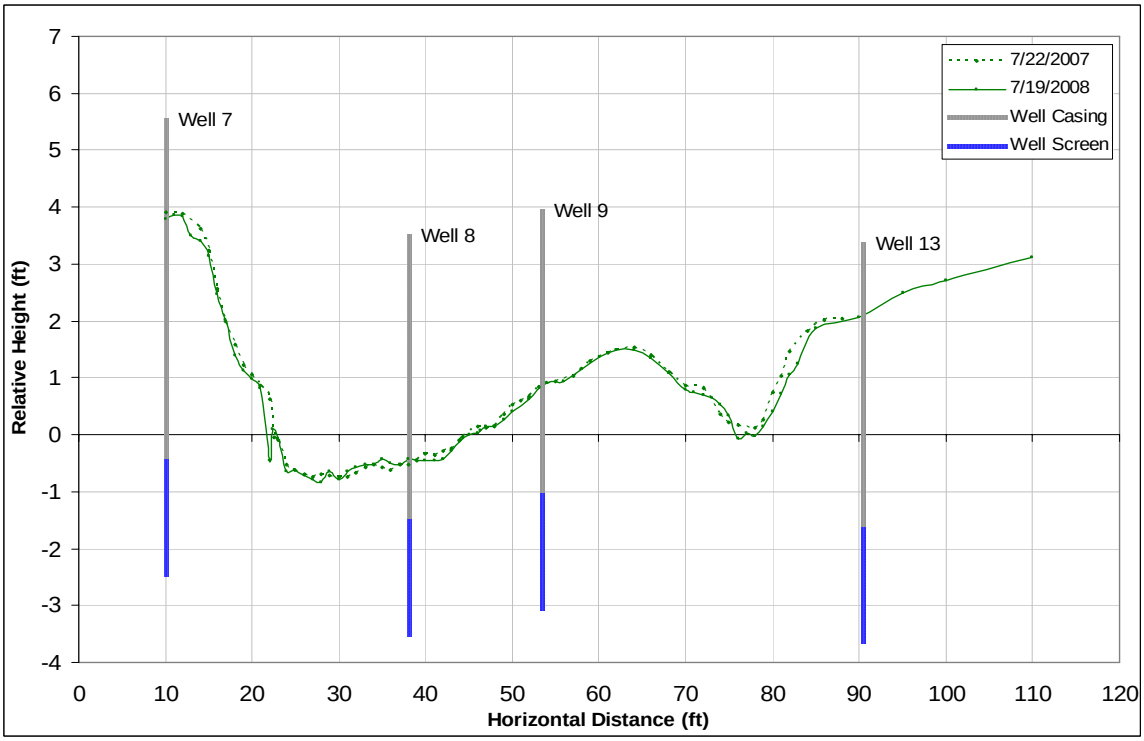

Figure 12. Well locations on transect 3; 20 feet downstream of transect 1. Green lines are surveyed cross-section dimensions at post-run off flows for 2007 and 2008. Base flow on 6/24/07 is 0 ft reference.

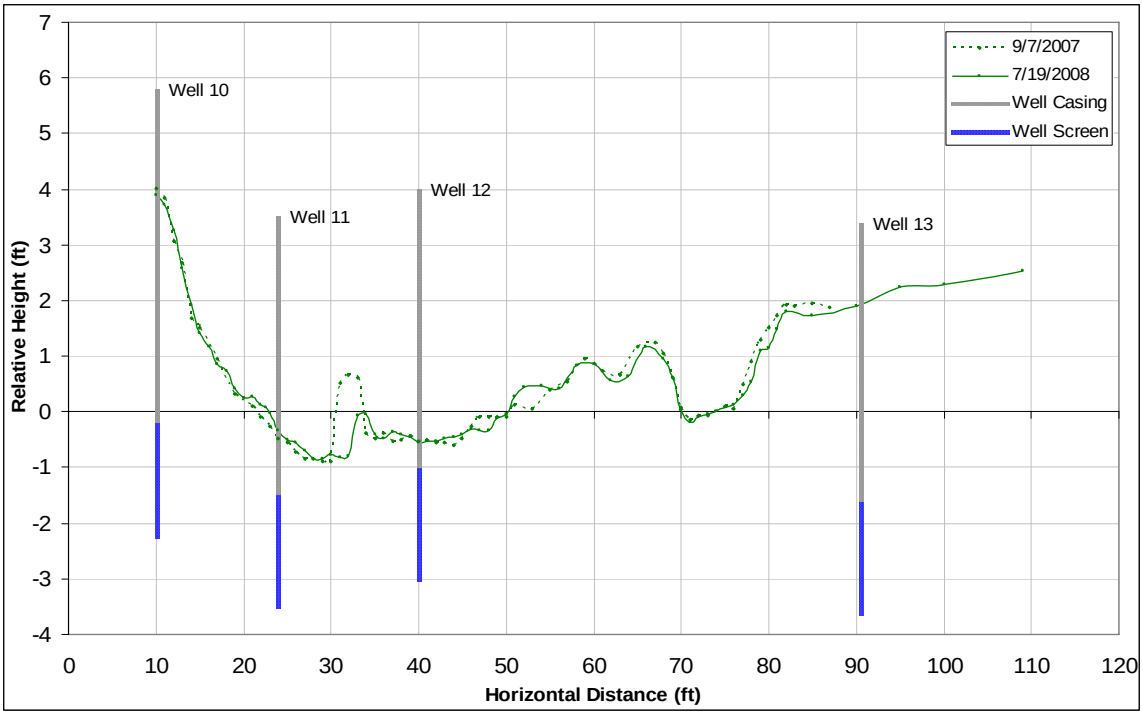

Figure 13. Well locations on transect 4; 30 feet downstream of transect 1 and the farthest downstream transect. Green lines are surveyed cross-section dimensions at post-run off flows for 2007 and 2008. Base flow on 6/24/07 is 0 ft reference.

A large event on December 1, 2007, according to the recovered equipment, destroyed all instream wells (Wells 2, 5, 6, 8, 11 and 12) and the stream gage. In May of 2008 one instream well was replaced. Well 5b was constructed as close as possible to the previous specifications and resulting data support a minimal change in the two wells.

Stream Stage Gauge

A stream stage gauge was established on transect 1 in the thalwag approximately 14 feet from well 1. The gauge was constructed of the same galvanized material with the exception of the screened interval. A T-coupling was added at the base of the riser to allow stream water to enter and act as a stilling well. A pressure transducer (Global Water

Instrumentation, Inc., WL16S Water Level Logger, accuracy – 0.01 ft / 0.2° F)[3] was added for real time stage and temperature measurements.

Water Levels

Water levels were determined using an electronic depth tape from the top of the casing. The relative water level below the surveyed top of casing could then be calculated to the site reference. Relative heights within the reach were determined using a construction survey scope (Dewalt Builders Level - DW090K) and staff gauge (accuracy - 0.25 in) with a large boulder on the left bank used as the ultimate reference. Water levels were collected during site visits on 6/24/07, 7/22/07, 9/7/07, 11/9/07, 1/4/08, 3/28/08, 5/9/08, 6/14/08, and 7/19/08.

One pressure transducer was dedicated as the stream stage monitor and one additional pressure transducer was moved from well to well to get higher time-based resolution.

Temperature Data

Each well was instrumented with a temperature data logger (Alpha Mach, iBCod Type 22L, accuracy - 0.9° F)[4] suspended to the top of the casing by twine. The data logger was set a few inches from the bottom of the screen (Figure 14).

[3] This is the product referenced when the term “pressure transducer” is used.
[4] This is the product referenced when the term “temperature data logger” is used.

Figure 14. Instrumenting an instream well.

The temperature data loggers were set to record between ½ hour and 2 hours depending on projected times between site visits. Additionally, two wells were instrumented with a pressure transducer for a limited period of time.

Recovered data loggers from the destroyed wells were later employed at different depths in wells 1, 3, 5b, and 14 to determine a temperature vertical profile.

Slug Tests

Slug tests were performed in the summer of 2008 using stream water. One gallon amber, glass containers were filled with stream water and allowed to set in the sun for 1 to 4 hours. A pressure transducer, programmed to record every second, was placed in the well

and temperature and water level were allowed to equilibrate. At equilibrium the well was filled as quickly as possible with the preheated stream water in the top of the casing. The instrumentation was removed when the water level retuned to within +/- 5% the original displacement.

Hydraulic-conductivity estimates were determined by the Bouwer and Rice (1976) method for slug test analysis in unconfined aquifers. The data was analyzed using spreadsheets, available from the USGS website (Halford and Kuniansky, 2002).

Analytical Modeling

The numerical model for a one-dimensional heat flow equation was adapted to predict the temperature at a given depth. The heat flow equation is given in Equation 1.

$$\frac{\partial T}{\partial t} = \frac{\lambda_x}{\rho_s C_s}\left[\frac{\partial^2 T}{\partial x^2}\right] - \frac{q_x n \rho C}{\rho_s C_s}\left[\frac{\partial T}{\partial x}\right] \qquad \text{Equation 1}$$

Where T is temperature, t is time, λ_x is the thermal conductivity, ρ_s is the porous medium density, C_s is the specific heat capacity of the porous medium, x is the depth, n is the porosity, q_x is the fluid Darcy velocity, ρ is the fluid density, and C is the fluid heat capacity. The heat flow equation given in Equation 1 assumes a flux over a constant volume.

Equation 1 is derived from the conservation of energy, where “the rate at which the total internal energy of the control volume changes is equal to the sum of the individual rates of change due to conduction, [and] convection…” (Deming, 2002).

The conductivity term refers to the conductive heat transfer to or from the control volume. The magnitude of this term for a given volume, i.e. constant λ_x, ρ_s, and C_s, is determined by the thermal gradient and direction is determined by the sign.

The advective term represents a heat transfer due to fluid flow which is a function of the Darcy velocity. The sign of the term depends on the direction of mass flux, i.e. mass leaving a given volume yields a negative term, mass entering a volume yields a positive term. For the analytical temperature predictions used in this study the advective term becomes positive for a losing reach and negative for a gaining reach.

Integrating the heat flow equation over time and space and selecting the thermal gradient as the surface water temperature and the residual ground water temperature from the previous time step, a semi-empirical equation is constructed. The semi-empirical equation (Equation 2) for the predicted groundwater temperatures used in this study becomes

$$T_{gw} = T_{gw(t-1)} + \frac{\lambda_x t}{\rho_s C_s x^2}\left[T_{sw} - T_{gw(t-1)}\right] + \frac{q_x n \rho C t}{\rho_s C_s x}\left[T_{sw} - T_{gw(t-1)}\right] \qquad \text{Equation 2}$$

Where T_{gw} is the ground water temperature at time (t) = t, λ_x is the thermal conductivity, ρ_s is the density and C_s specific heat capacity of the porous medium, x is the depth of the temperature probe, T_{sw} is the measured surface water temperature, n is the porosity, q_x is the fluid Darcy velocity, ρ is the fluid density, and C is the fluid heat capacity.

The constants used in the calculation were the values for liquid water and saturated Tottori sand (Table 2) reported by Stonestrom and Constantz (2003).

	Density	Porosity	Specific Heat Capacity	Thermal Conductivity
	kg/m^3	V_{pores}/V_{bulk}	J/kg °C	W/m °C
Liquid water	1000	n/a	4200	0.60
Porous Medium	1830	0.31	2600	2.2

Table 2. Constants used in analytical temperature estimation

The fluid Darcy velocity (q_x) was selected to create the best fit to the observed ground water temperatures by adjusting the hydraulic gradient (*dh/dl*). The hydraulic conductivity (*K*) was determined from the temperature-dependant Muskat equation (Equation 3) and using the experimentally measured intrinsic permeability from the slug tests.

$$K = kg\frac{\rho}{\eta} \qquad \text{Equation 3}$$

Where *k* is the intrinsic permeability, *g* is the acceleration due to gravity, ρ is the fluid density at the surface water temperature, and η is the dynamic viscosity at the surface water temperature. Both the density and dynamic viscosity are temperature sensitive.

Table 3 lists the *K* values calculated using the Muskat equation at different temperatures and at the given intrinsic permeability (*k*) = $1.88 * 10^{-10}$ ft^2.

T (°C)	T (°F)	K (ft/s)	% Change
0	32	3.16E-04	
5	41	3.27E-04	17.7%
10	50	4.32E-04	16.2%
15	59	4.95E-04	14.7%
20	68	5.62E-04	13.6%
25	77	6.32E-04	12.4%
30	86	7.05E-04	11.5%

Table 3. Calculated hydraulic conductivities (K) at different temperatures and at a given intrinsic permeability (k) = $1.88 * 10^{-10}$ ft^2.

The boundary conditions for $T_{gw}(x,t)$ are:

$T_{gw}(0,t) = T_{sw}(t)$

$T_{gw}(x,0)$ = first measured ground water measurement

The very low sensitivity to errors in the estimated thermal properties is the result of the large volumetric heat capacity (the product of the density and specific heat capacity of the porous medium) in the denominator of both the advective and conductive term. This relationship yields such small values that an error of +/- 300% in the estimations would translate into a +/- 1° F error in the predicted temperature only for temperature gradients of hundreds of degrees or time steps of weeks.

IV. Results and Discussion

Stream Stage and Subsurface Water Levels

The water levels measured during site visits were found to be nearly equal and fluctuated congruently with the stream stage. The largest head difference was 0.25 feet between wells and between the wells and the stream stage suggesting an extremely responsive system (Figure 15). The average hydraulic gradient from the top of the reach to the bottom of the reach was found to be 0.003 ft/ft. Multiplying this value by the hydraulic conductivity measured in the slug tests, the Darcy velocity in the horizontal direction is calculated to be 5.1 x 10^{-7} ft/s. All stage and head values are measured relative to the stream stage (0.0 ft) on 6/24/07.

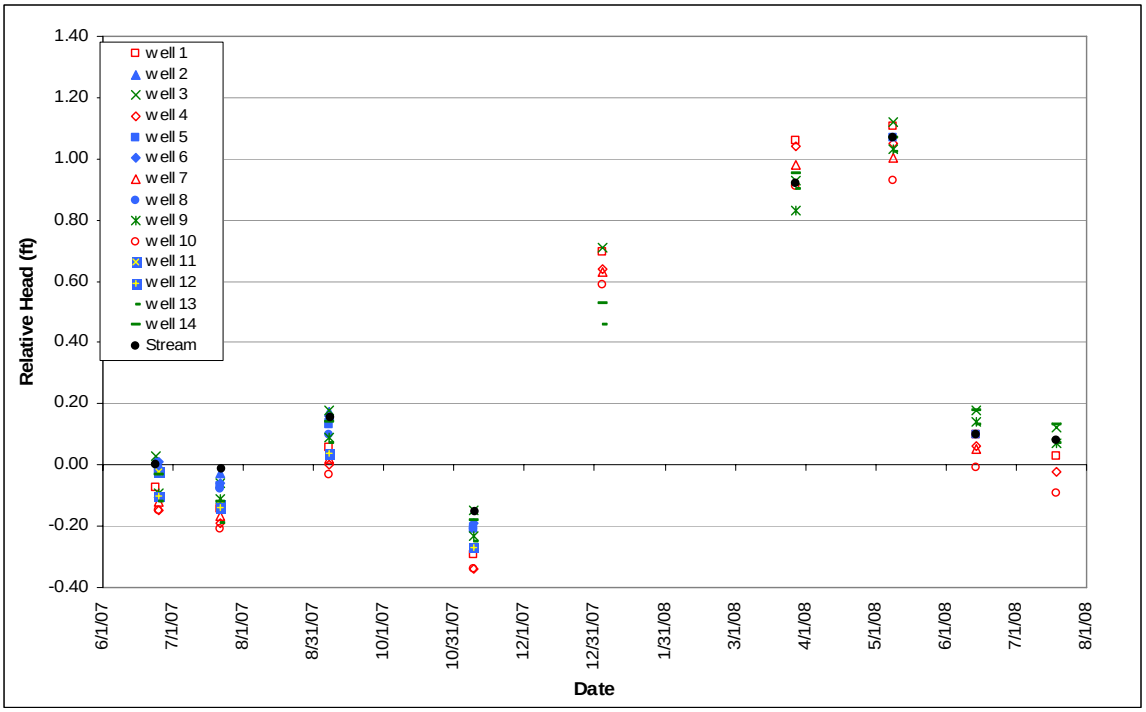

Figure 15. Measured water levels from each site visit. Left bank wells are open, red marks, right bank and floodplain wells are green ticks, instream wells are closed, blue marks and the stream stage is a closed, black circle.

The water levels indicate a strong snow-melt driven system. The annual flow regime can be classified into 3 categories. The first is monsoonal appearing in late July and receding in early October. The second is snowmelt runoff beginning in March and running into June. The final regime is the base flow period occurring between snow-melt and monsoons. The characterizations that lead the following discussions are depicted graphically in Figure 16.

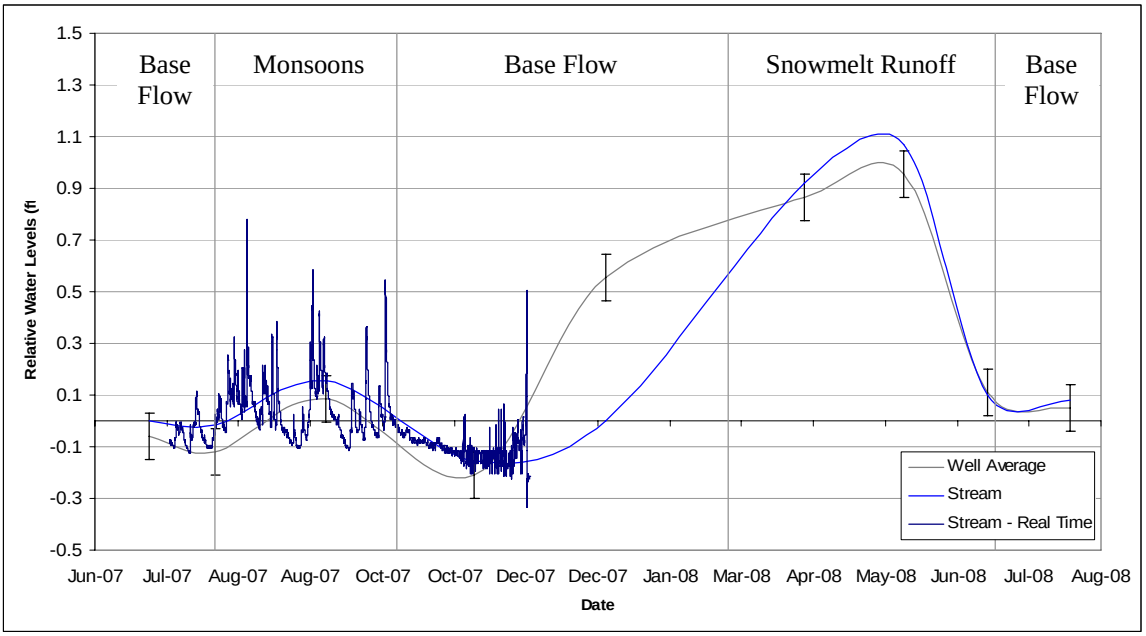

Figure 16. Average well water levels and stream stage data. Note the January 4, 2008 stream stage value is estimated as ice prevented an accurate measurement.

Water levels collected during site visits indicate that ground water generally flows down-valley and from the right bank to left bank between snowmelt runoff events and left to right during snowmelt runoff. Figure 17 is a collection of ground water level contour maps showing gaining and loss potentials. Contours were constructed from Kriged water level data collected during site visits. It is presumed that the left bank receives some groundwater from the catchment to the south and west (Figure 3), which at lower elevations, would gain melt water earlier and dissipate sooner than stream water derived from the higher elevation source.

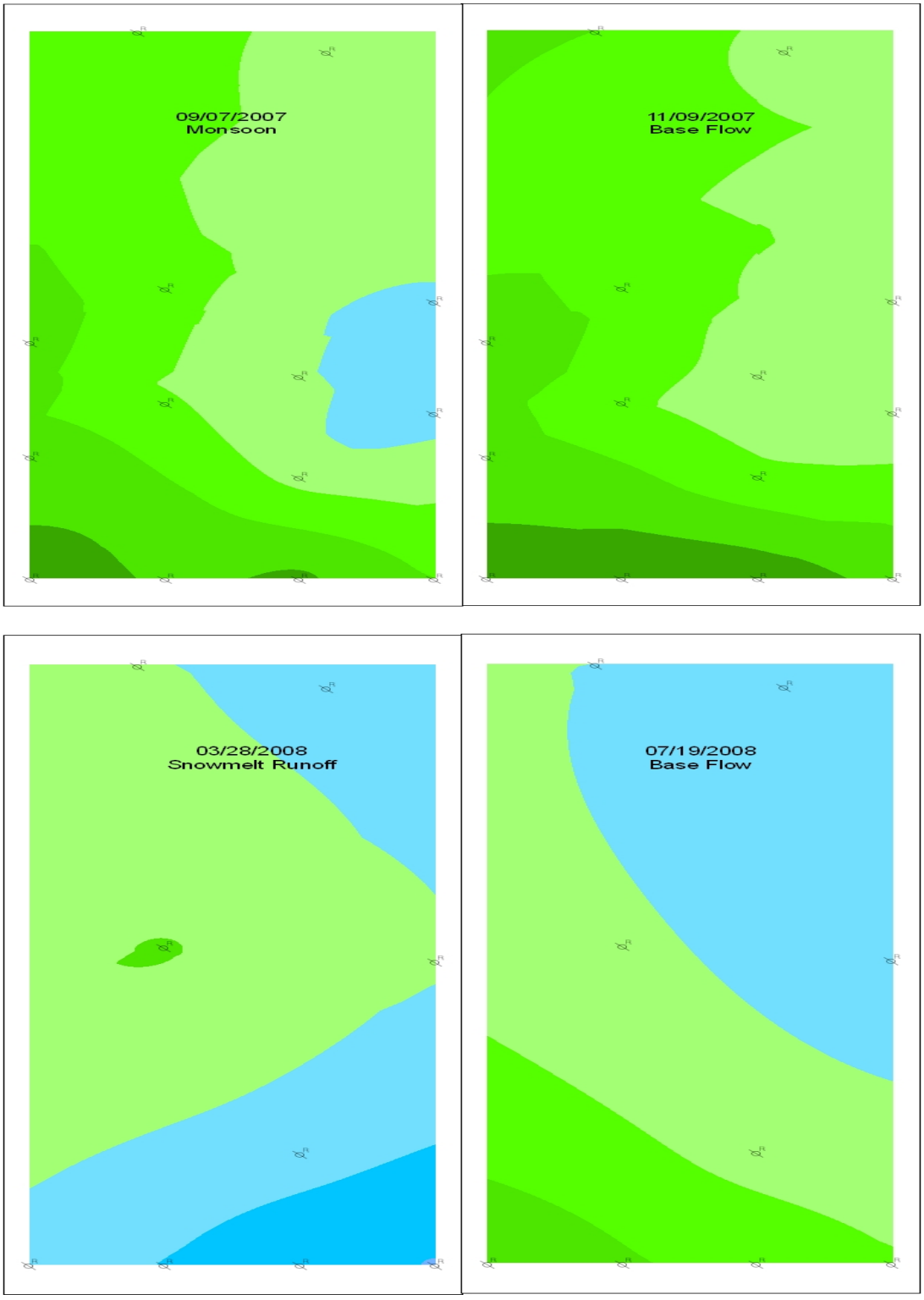

Figure 17. Ground water level contour map relative to stream stage. Contours are 0.05 ft (approximately 1.5 cm) with green indicating potential loss from stream and blue indicating potential gain to stream. Bottom of map represents river left with stream flow from right to left. Note that data are missing from instream wells for the 2008 water levels.

The idea that the subsurface is extremely responsive to changes in the stream stage was demonstrated by placing a pressure transducer in two instream wells. The pressure transducer was first placed in an instream well on the first transect, well 2 (Figure 18). This period was characterized by the tail end of the monsoon season and the start of a low flow period. The second time period included the low flow period in an instream well (well 11) at the downstream end of the reach (Figure 19). The period ended with a large event that destroyed all the instream wells.

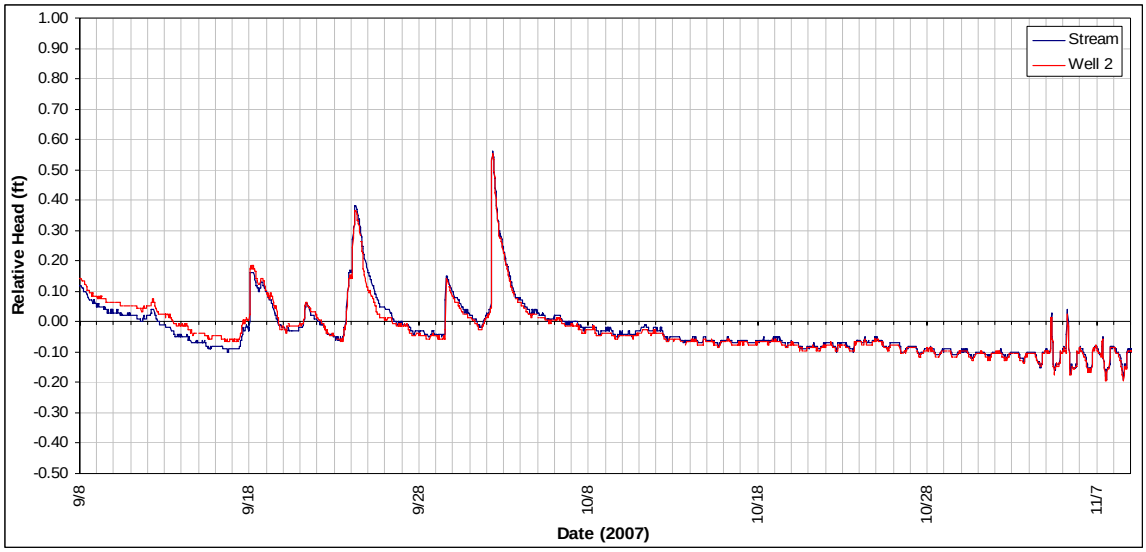

Figure 18. The relative head difference between the stream stage and instream well water level. Note the response to precipitation events in September and the diurnal fluctuations in October.

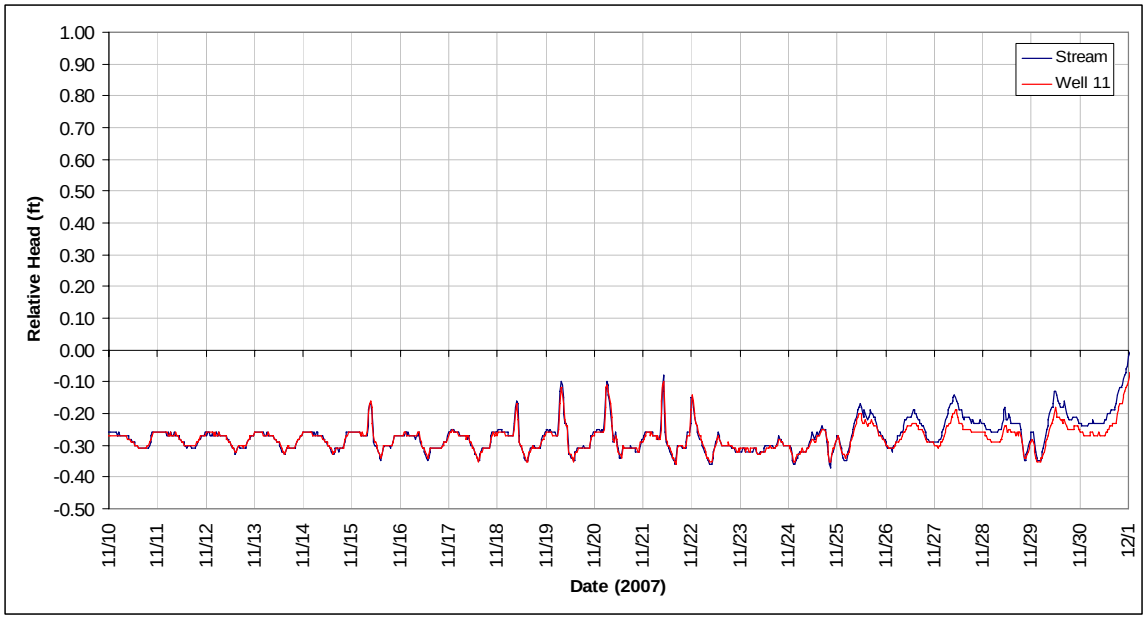

Figure 19. The relative head difference between the stream stage and instream well water level.

Hydraulic Conductivity

An experiment was performed to measure the hydraulic conductivity of the porous medium using a slug test. Figure 20 shows the return to static water level after the positive displacement slug test.

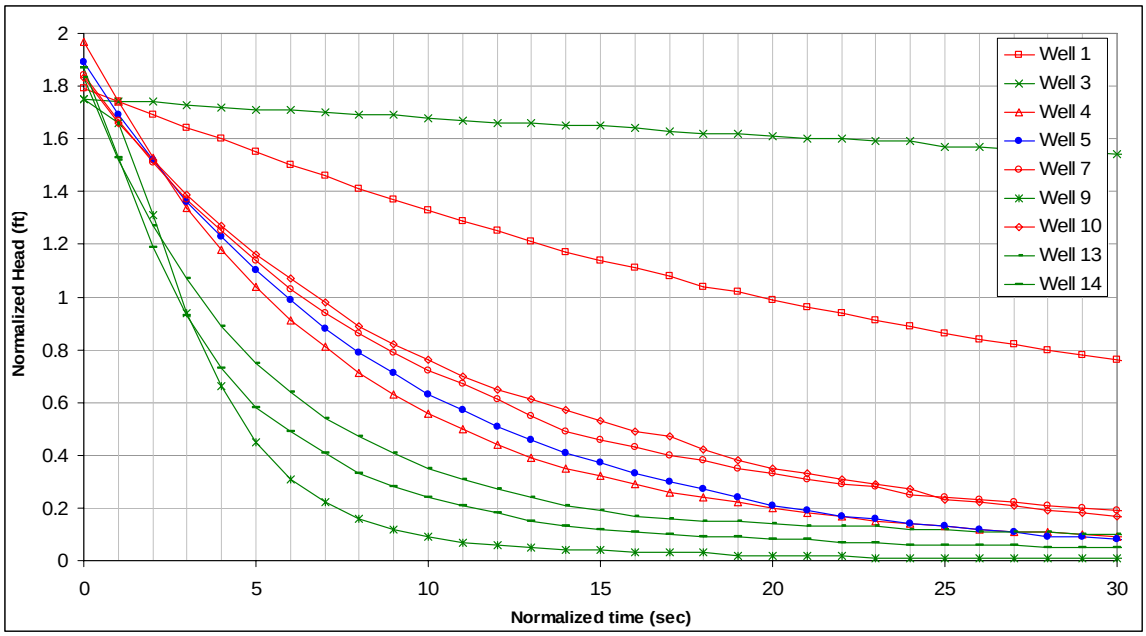

Figure 20. The head change over time of wells that were slug tested. Green lines with ticks represent right bank and floodplain wells, red lines with open marks represent left bank wells and the blue line with closed marks represent a reconstructed instream well. Zero head is the starting water level.

The right bank as a whole had higher hydraulic conductivities than did the left bank. It is worth noting that the two slowest responding wells were located in the first transect suggesting an additional control on the groundwater regime through the reach. The slower response of the left bank wells is thought to be the result of a smaller grain size as noted in the exposed surface of the cut bank. Smaller gain sizes, in alluvial deposits, indicate slow moving water. The results of the slug test along with clasts placement and size observations (see Channel Description section in the Introduction) suggest that the current channel has only recently occupied its current position. With this in mind it appears very likely that the larger clasts surveyed in the stream channel do not go very deep, and therefore the instream well displays a similar hydraulic conductivity as the left bank wells. The lower conductivity values in transect 1 may be the result of a slower stream current dropping out fines at the top of the reach.

The Bouwer and Rice (1976) estimated hydraulic conductivity values for the reach are reported in Table 4.

Well	ft/sec	m/sec
Well 9	5.5E-04	1.7E-04
Well 14	2.9E-04	8.8E-05
Well 13	2.5E-04	7.6E-05
Well 4	1.8E-04	5.5E-05
Well 5b	1.7E-04	5.2E-05
Well 7	1.6E-04	4.9E-05
Well 10	1.6E-04	4.9E-05
Well 1	4.6E-05	1.4E-05
Well 3	7.7E-06	2.3E-06

Table 4: List of measured hydraulic conductivities in descending order.

The estimated values agree with reported values (Schwartz and Zhang, 2003) for a sand/gravel alluvial aquifer. Average values are reported in Table 5.

Aquifer Material	ft/sec		m/sec	
	high	*low*	*high*	*low*
Gravel	9.8E-02	9.8E-04	3.0E-02	3.0E-04
Coarse Sand	2.0E-02	3.0E-06	6.0E-03	9.0E-07
Medium Sand	1.6E-03	3.0E-06	5.0E-04	9.0E-07
Fine Sand	6.6E-04	6.6E-07	2.0E-04	2.0E-07
Slit, Loess	6.6E-05	3.3E-09	2.0E-05	1.0E-09
Till	6.6E-06	3.3E-12	2.0E-06	1.0E-12
Clay	1.5E-08	3.3E-11	4.7E-09	1.0E-11

Table 5: Average reported values for unconsolidated sedimentary material.

Ground Water Temperatures

Groundwater temperatures were collected by a temperature data logger at 0.5 to 2.0 hour intervals for all wells within the reach. The data retrieved suggest a more complicated system than that which might be deduced from the relative heads reported above.

The left bank temperature profile appears to be nearly independent of other ground water in the reach. The temperature shows a strong annual signature with only a few short term

trends appearing. The signature is characteristic of either a very deep and thus buffered temperature regime or a gaining reach. The lack of a strong hydraulic gradient (dh/dl) from the stream averaging 0.02, 0.02, 0.01, and 0.01 ft/ft for well 1, 4, 7 and 10 respectively suggests little flux that would be thermally buffered as with depth. Figure 21 shows the left bank temperature profiles along with the stream daily average temperature.

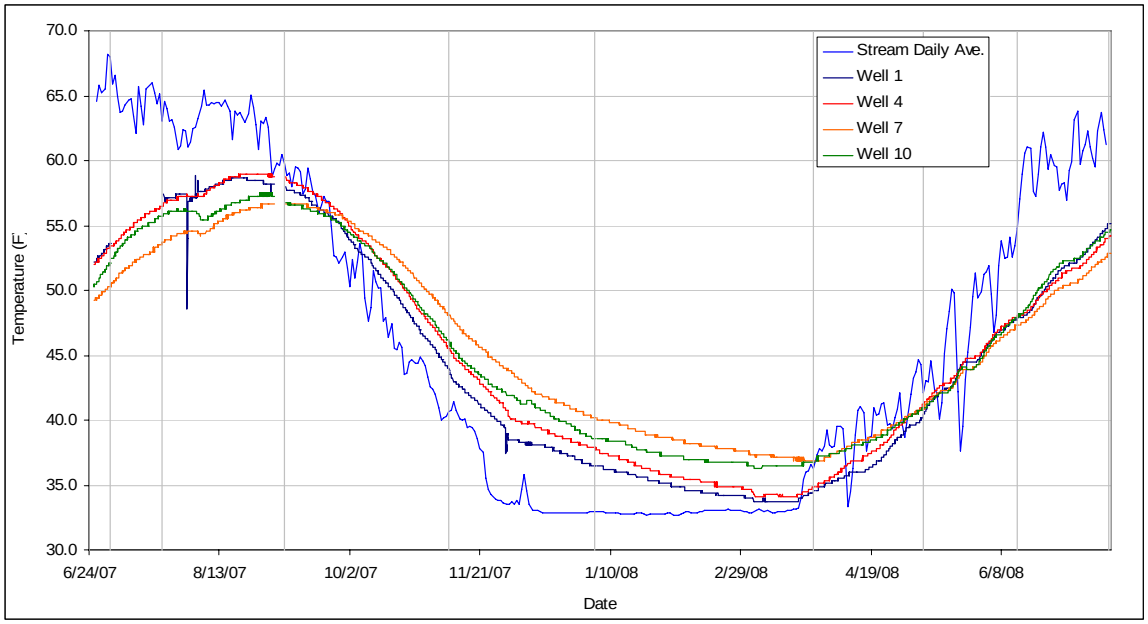

Figure 21. Left bank temperature profiles over time. Vertical grid lines denote site visits.

The right bank appears to have much more connectivity. There are no diurnal signatures in the right bank but large multi-day temperature shifts appear with varying degrees of amplitude and delay in the temperature profiles. The difference in the temperature signals in the left bank and right bank and floodplain is most likely due to a conductive heat transfer. The wells on the left bank are buried to a depth of approximately 4 feet, while those on the right bank are buried between 1 to 2.5 feet (Figures 10 to 13). The wells on river right are also closer to open water (wells 3 and 9 to the stream and wells 13 and 14

to the abandoned channel). Figure 22 shows the right bank temperature profiles along with the stream daily average temperature.

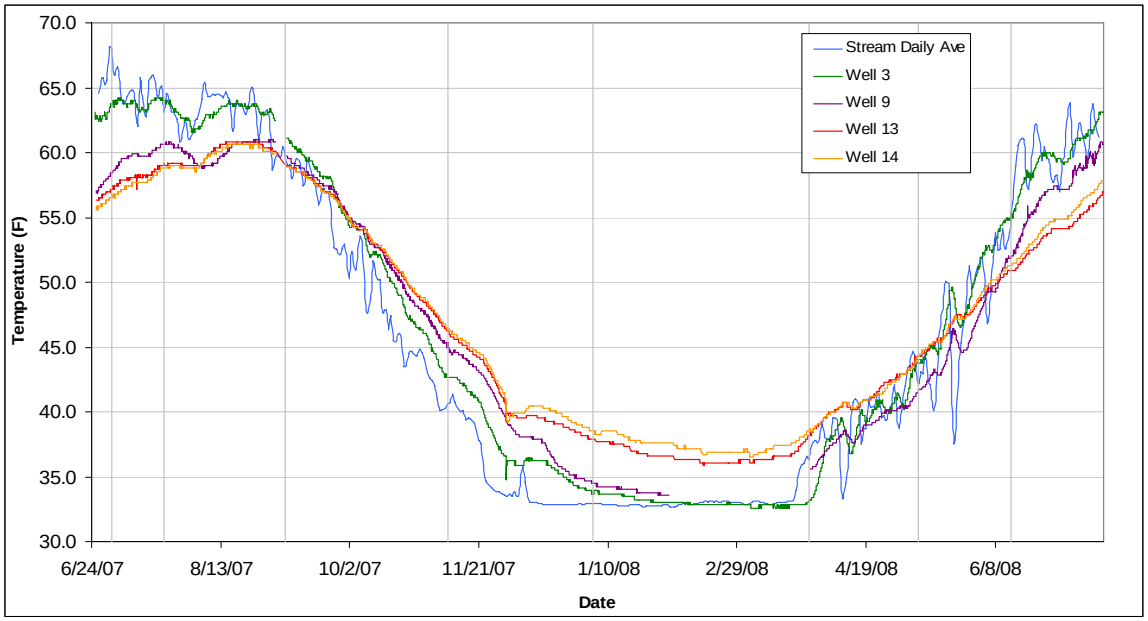

Figure 22. Temperature profile of right bank and floodplain wells. Vertical grid lines denote site visits.

The instream wells show varied temperature signals depending on seasonal flow, the well's location in the stream course and depth of the instrument. Only two wells (well 5 and well 12) of the six are presented in order to minimize congestion. Well 2, well 6, and well 8 displayed responses that were similar to wells 5 and 12. The well 11 thermograph was very similar to the stream thermograph indicating a strong loss from the stream.

The following figures, 21, 22, 23, 24, and 25, show representative thermographs of the 2007 post-runoff base flow condition, 2007 monsoons, 2007 post-monsoon conditions, 2008 runoff and 2008 post-runoff flow conditions, respectively.

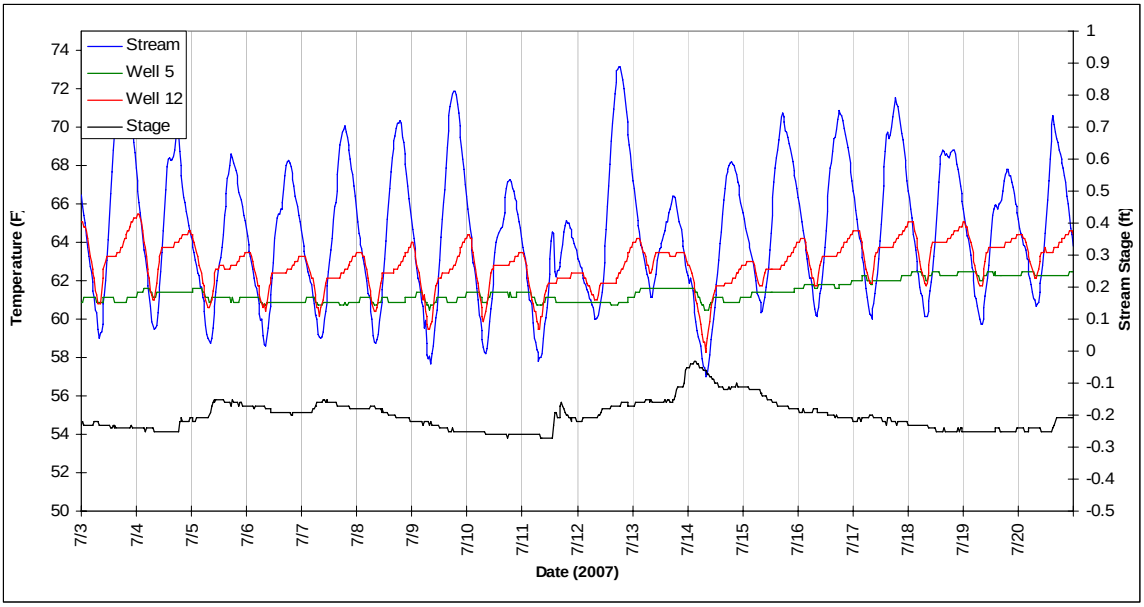

Figure 23. Snapshot instream wells' temperature signature during 2007 post-runoff base flows.

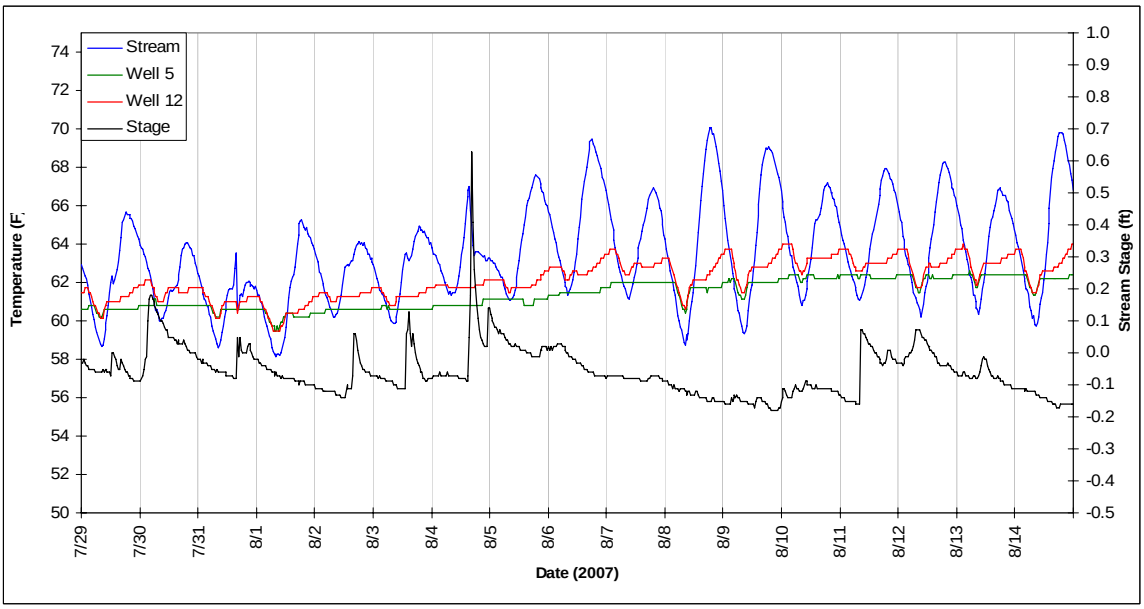

Figure 24. Snapshot of instream wells' temperature signature during 2007 monsoon events and higher base flow.

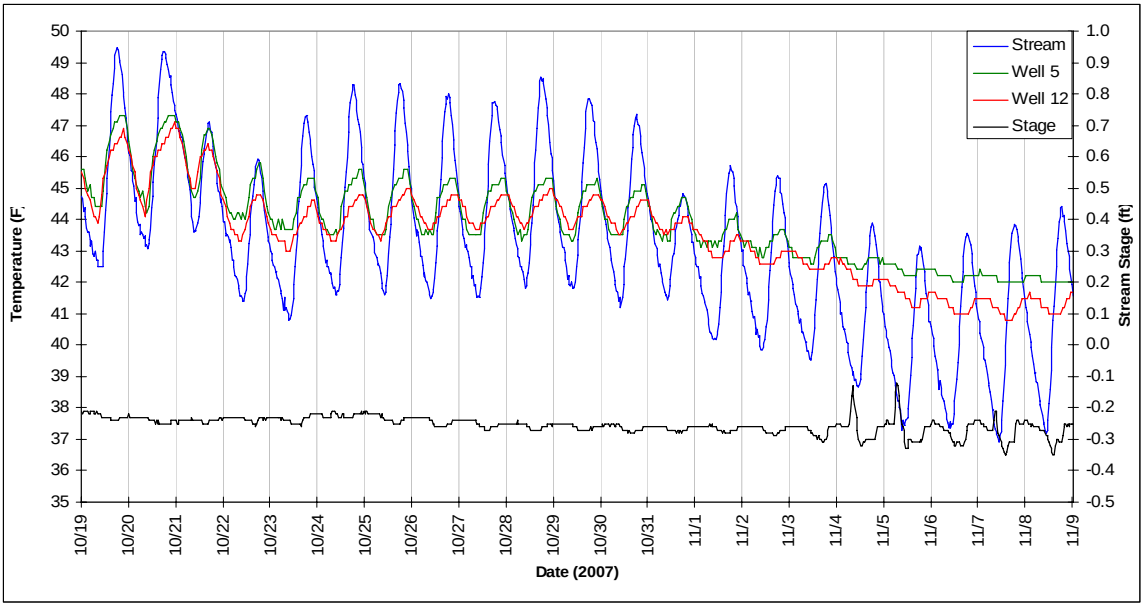

Figure 25. Snapshot of instream wells' temperature signature during 2007 post monsoon base flows.

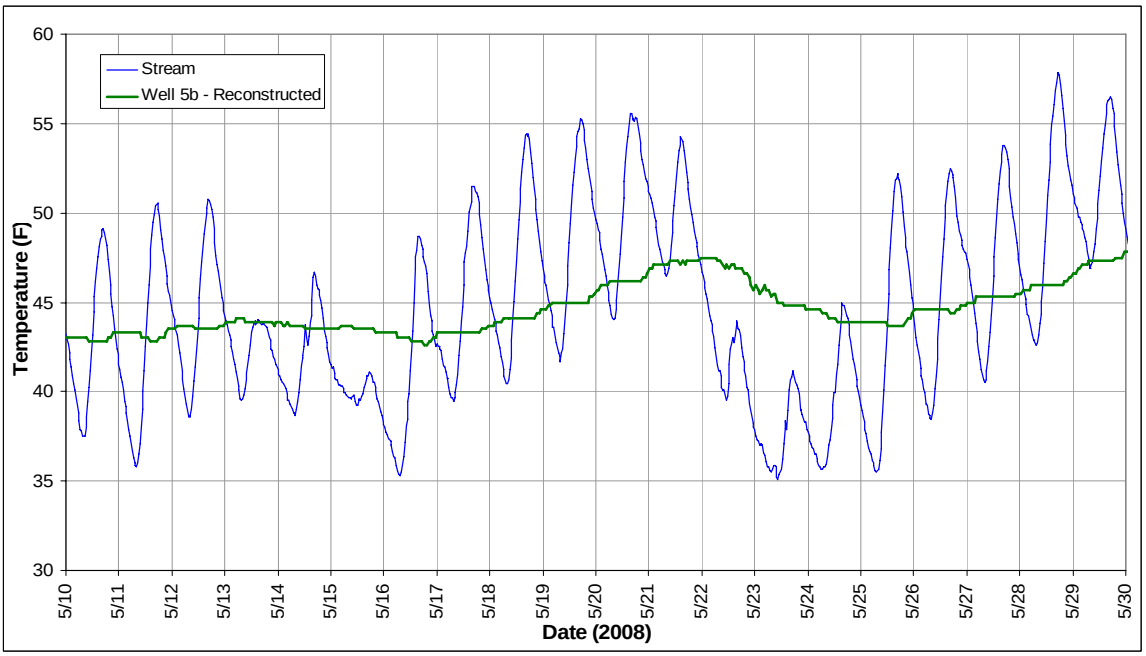

Figure 26. Snapshot of instream well's temperature signature during 2008 runoff. Well 12 was lost in the December 1, 2007 event as were all other instream wells.

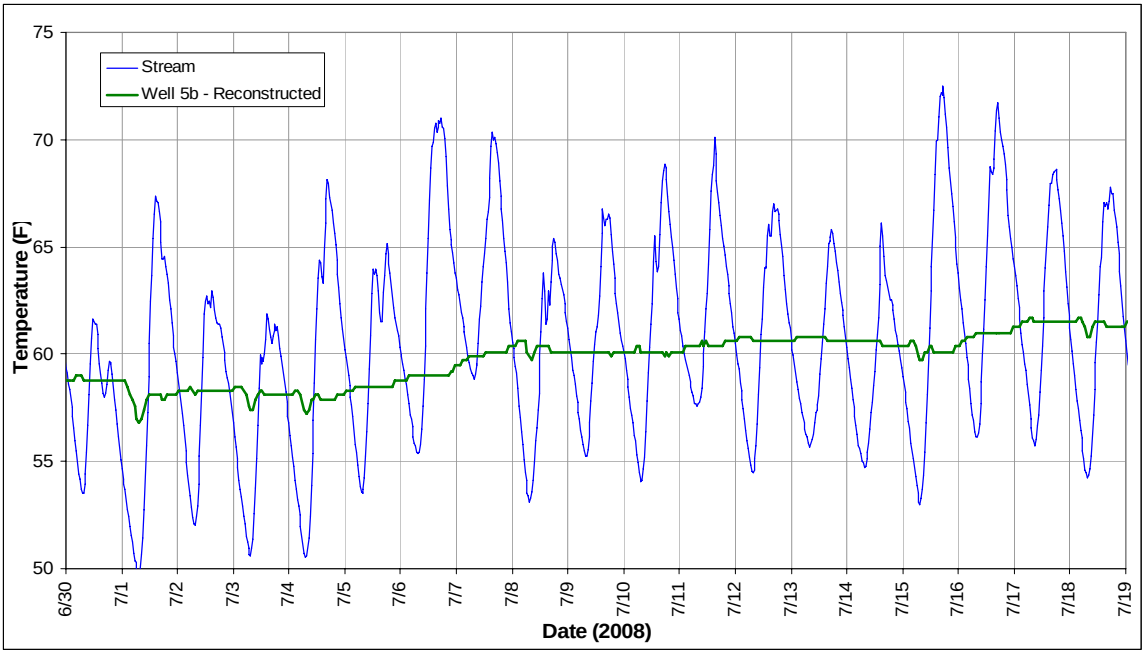

Figure 27. Snapshot of instream well's temperature signature during 2008 post runoff base flows.

With the exception of runoff, the temperature signals at depth display characteristics of a losing reach and a gaining reach. This combination not only appears from well to well and at depth, but also appears to have some diurnal control. In well 5/5b this generally appears as a small, quick temperature drop and recovery in the early morning where stream temperatures are coolest. In well 12 the profile may be described as a flat line within a quasi - sin wave. In all cases this occurs on the rising limb of the temperature curve.

In a losing reach, it is presumed that at greater depths one finds a reduced amplitude and increased lag times in the diurnal temperature signal. Conversely, in a gaining reach the temperature at any depth would be more or less constant and uniform on a daily time scale. The instream wells within this particular reach appear to have components of both and to varying degrees depending on specific location.

Diurnal stream discharge patterns, that reduce discharge during the afternoon, have been widely observed as a response to evapotranspiration (ET) (Henry et al. 1994). Constanz et al. (1994) demonstrated that these discharge patterns may also be a function of the stream temperature itself. According to the Muskat equation (Equation 3), the hydraulic conductivity of bed material is dependant upon the temperature of the fluid, thus as the stream temperature cools one expects to see less loss in a losing stream reach. This would, of course, not be the case in a gaining reach due to the relative uniform temperature of the ground water.

The expected results from a decrease in the stream temperature on a losing reach may include: 1. decreased subsurface flux at the monitoring site, resulting in less thermal response to cooler stream temperatures, 2. decreased subsurface flux upstream of station resulting in an increase in discharge, with a change in the cross-sectional profile between upstream and downstream enhancing or negating the reduced flux on the monitoring station, 3. a decreased subsurface flux upstream may reduce a deeper ground water flux at the monitoring station, effectively increasing hydraulic gradient between it and the stream stage, or 4. some combination of the three.

Vertical Gradient

To resolve the cause of these thermal responses, a temperature profile with depth was determined by placing temperature data loggers at several depths within several wells. Figure 26 is the resulting thermograph of the reconstructed instream well 5b.

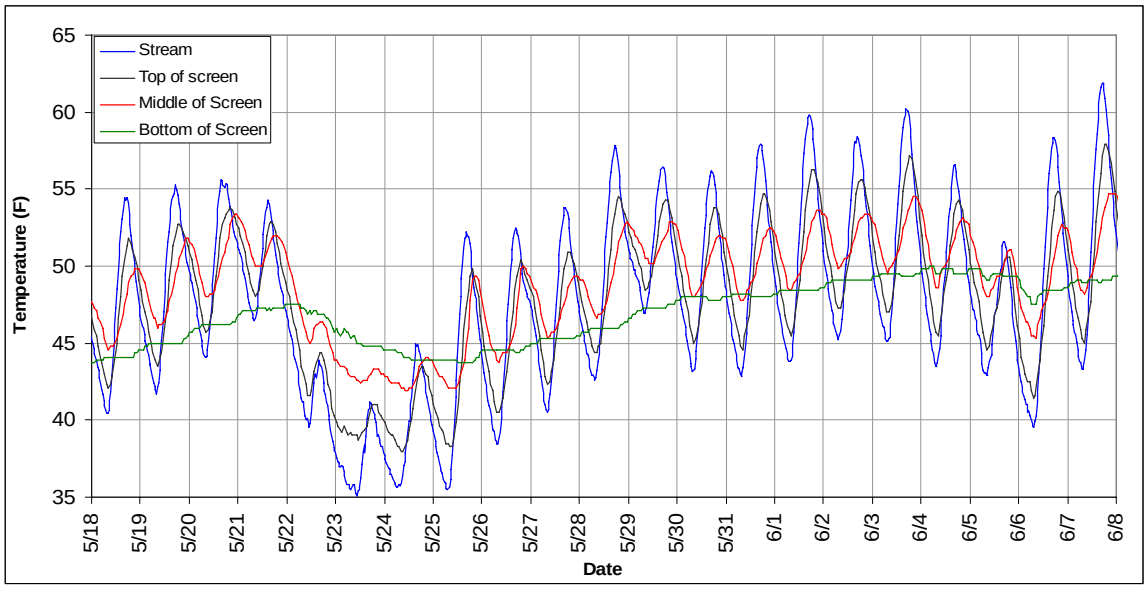

Figure 28. Temperature profiles of the top of the screen, the middle of the screen and the bottom of the screen in well 5b during runoff in 2008.

In the temperature profile displayed above, we see what is presumed to be a strong losing stream at the upper sections of the screened interval and a departure from that classic profile at the bottom of the screen. This would suggest that there may be a strong resistance to vertical flow, a defined layer of low conductivity or that the deepest temperature probe intersects an independent ground water flow path.

One key point to note in the above thermograph is subsurface temperature response during the sharp decline in surface water temperatures of 5/22/08 to 5/25/98. The deeper groundwater temperatures were able to maintain temperatures higher than the shallower temperature probes suggesting an inversion or well water mixing is unlikely, at least under certain flow conditions. This is not to say that there is no thermal influence within the well, as reported earlier the slow Darcy velocity in the horizontal direction would allow for conductive thermal exchange in the well water.

Analytical Solution

In order to compare the vertical gradient results with the expected responses, the analytical heat equation was adapted, as described in the methods section. The predicted responses offer insight into the thermal and hydrologic system controls. Figures 29, 30, and 31 show the analytical results for three depths in well 5b during runoff conditions. Figures 32, 33 and 34 show the analytical results for post runoff, baseflow conditions.

The amplitude of the subsurface response is dictated primarily by the flux and the time of response is primarily dictated by depth.

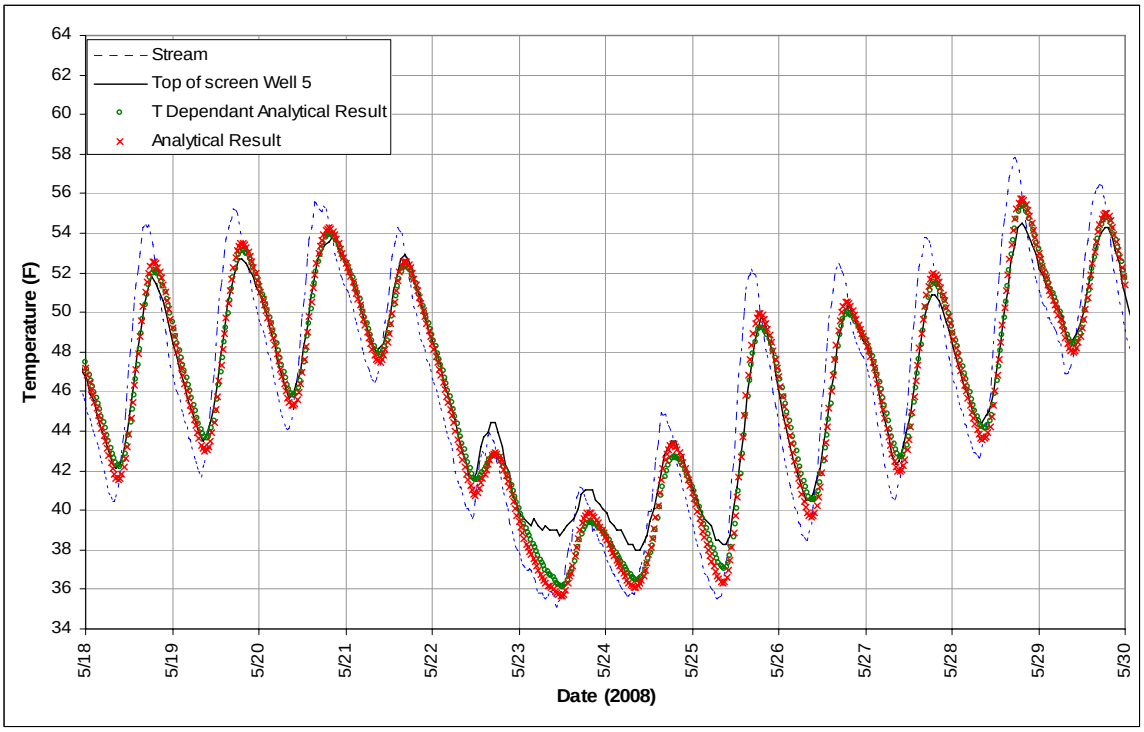

Figure 29. Graph depicting stream and well temperatures with the corresponding analytical predictions with and without temperature compensation. Depth = 1.0 ft, q = 1.60 x 10^{-4} ft/s. This graph represents runoff conditions.

The temperature-dependent results include a temperature-dependent hydraulic conductivity derived from the intrinsic permeability measured in the slug tests and the

temperature-based density and viscosity functions. The temperature-based results should yield a more accurate depiction, and will be the only results reported below.

The departures from the predicted temperature at the top of the screen (Figure 29) are minimal and may be characterized as just missing the minimum and/or maximum predicted ground water temperature.

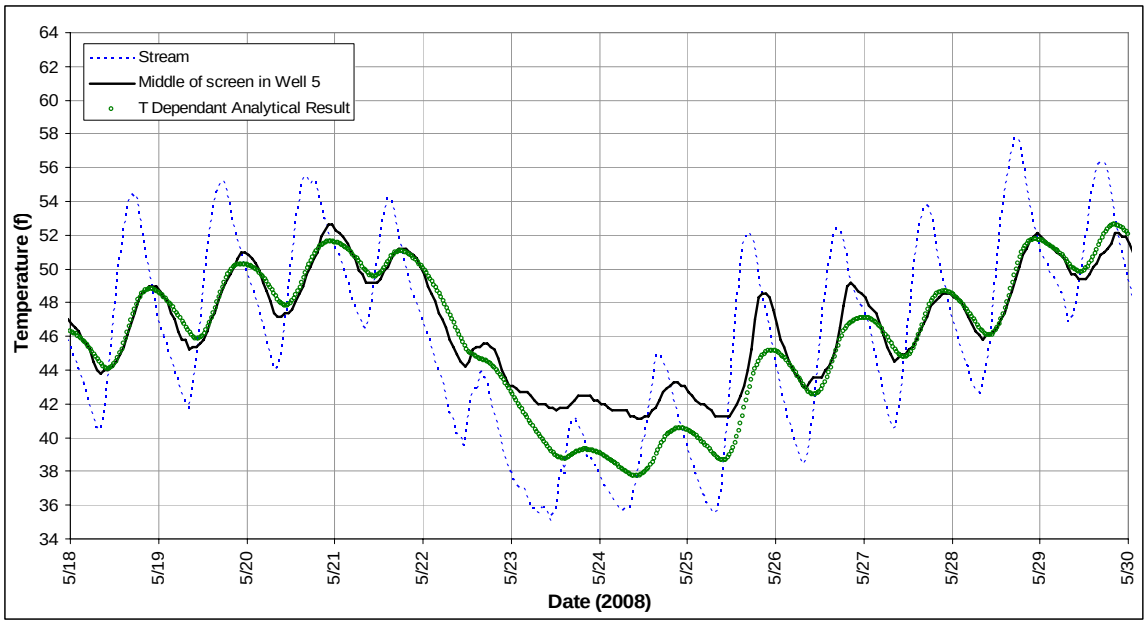

Figure 30. Graph depicting stream and well temperatures with the corresponding analytical predictions with temperature compensation. Depth = 2.0 ft, q = 1.07 x 10^{-4} ft/s. This graph represents runoff conditions.

The departures from the predicted values in the middle of the screened interval (Figure 30) are more pronounced as the depth increases and the best fit mass flux value was slightly lowered, but lag times are similar. The larger departures in the predicted temperature from the observed temperature, especially on May 23, 24 and 25, are likely due to the application of equation 2. In equation 2 the temperature difference at a given

depth (x) is the difference in stream temperature and the predicted ground water temperature at time (t) = $t - 1$. It is likely that as the temperature falls, in this case, the ground water temperatures at lower depths are warmer (Figure 28) and would yield a change in the thermal gradient (dT/dx) in both the conductive and advective term.

At the bottom of the screen the lag times become consistently later and the flux had to be significantly lowered to achieve a reasonable relationship with predicted temperature fluctuations.

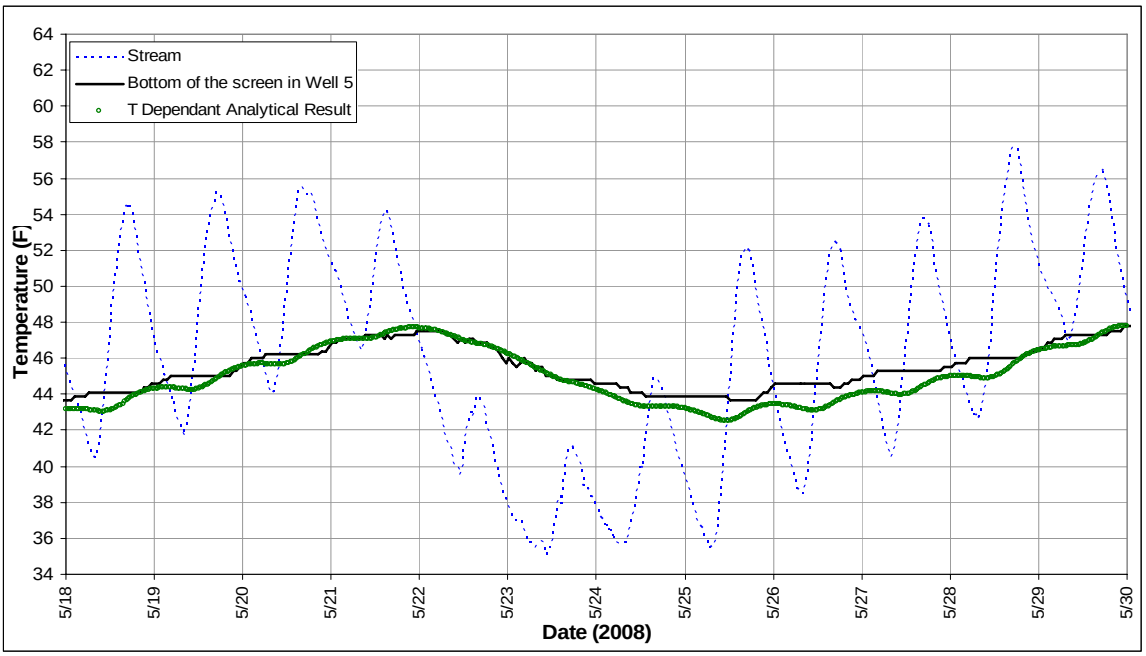

Figure 31. Graph depicting stream and well temperatures with the corresponding analytical predictions with temperature compensation. Depth = 3.0 ft, q = 1.89 x 10^{-5} ft/s. This graph represents runoff conditions.

The departures at the bottom of the screen in well 5b to the predicted values suggest a source from outside the stream water in the study reach.

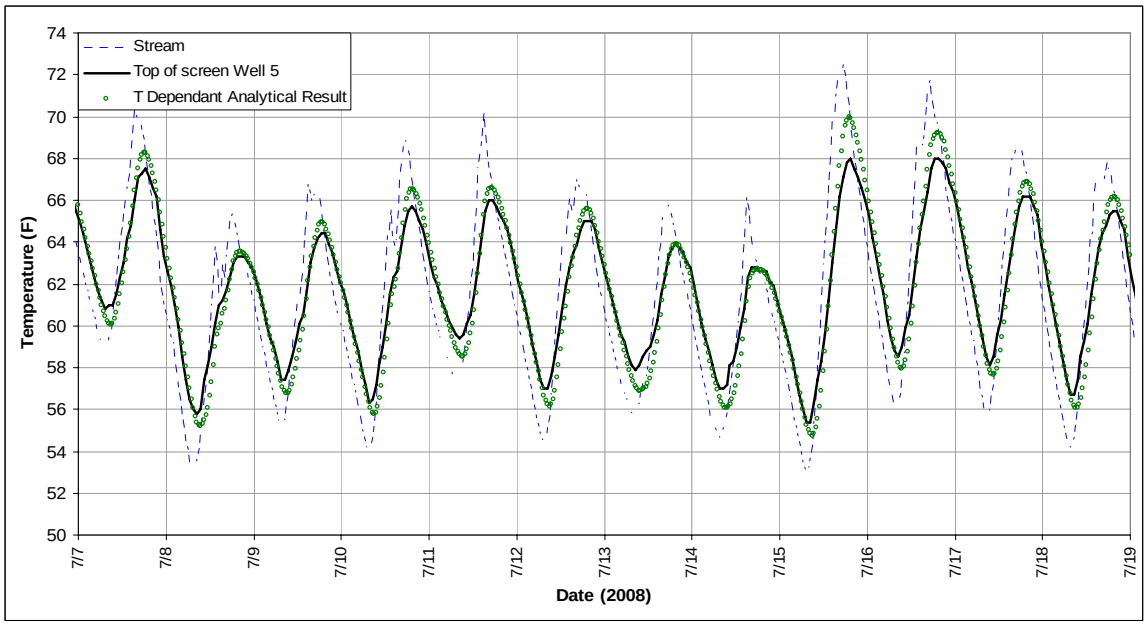

Figure 32. Graph depicting stream and well temperatures with the corresponding analytical predictions with temperature compensation. Depth = 1.0 ft, q = 1.60 x 10^{-4} ft/s. This graph represents baseflow.

Again the measured temperature values in the top of the screen (Figure 32) agree reasonably well with the predicted values at the same flux rate.

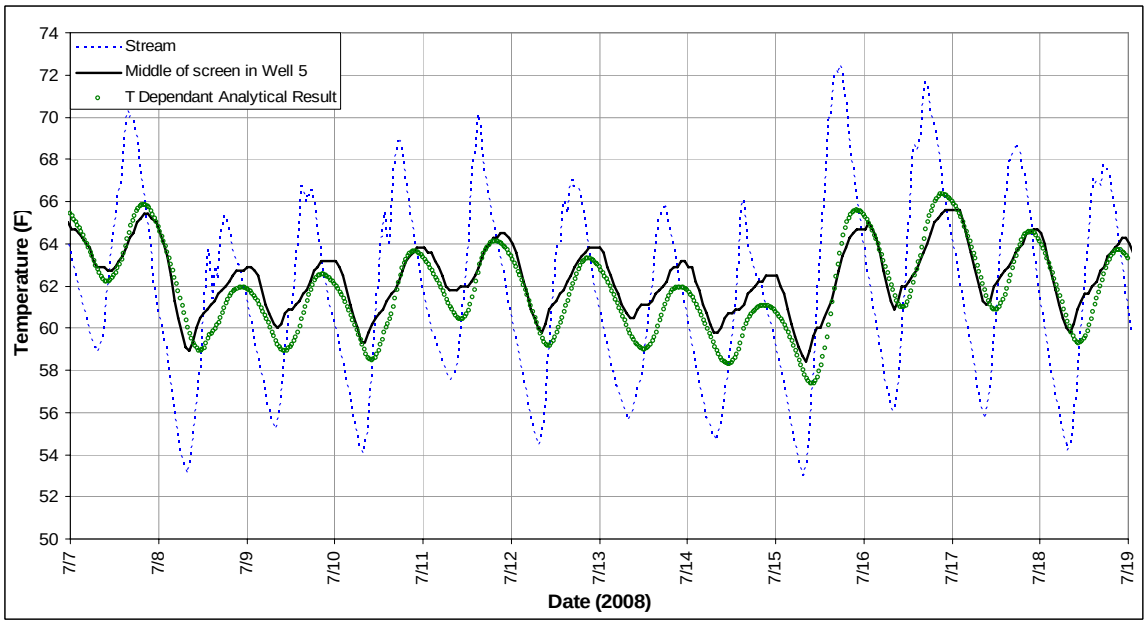

Figure 33. Graph depicting stream and well temperatures with the corresponding analytical prediction with temperature compensation. Depth = 2.0 ft, q = 1.07 x 10^{-4} ft/s. This graph represents baseflow.

The departures for the middle of the screen temperature values are still not high, but the departures become consistent each day. The measured temperatures display lag times and rates of change that are predicted with the simple 1-D system, but these temperatures appear to be "pushed" by an external source at relatively regular intervals. We also begin to see the unconventional rebound from low temperatures that appear in well 12 (Figures 23 and 24).

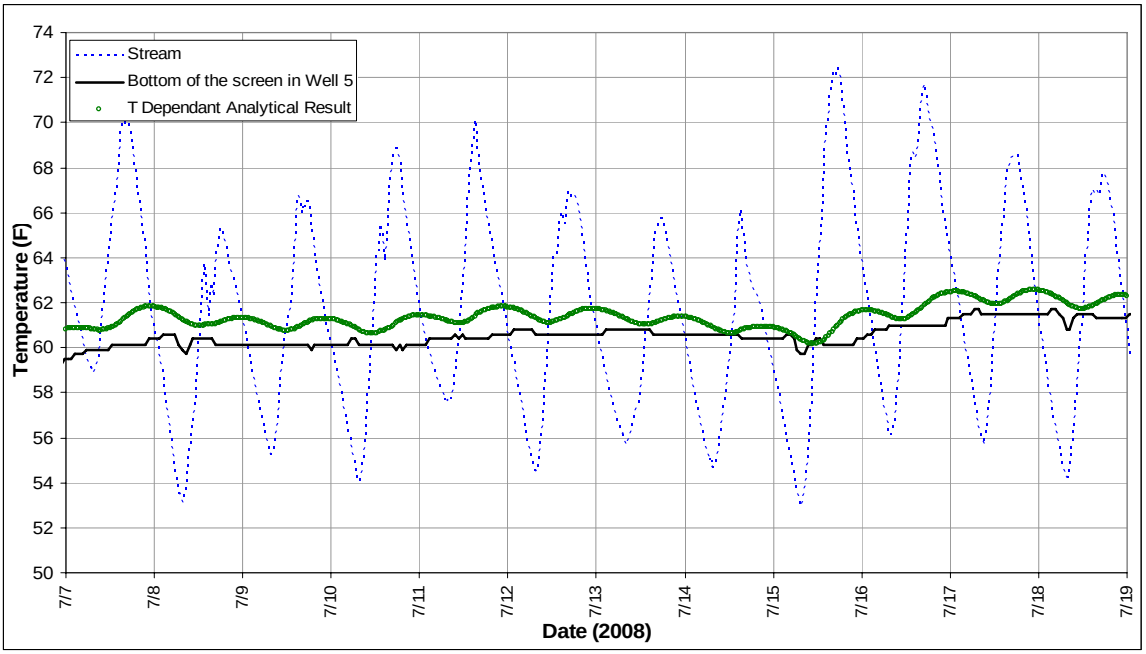

Figure 34. Graph depicting stream and well temperatures with the corresponding analytical predictions with temperature compensation. Depth = 3.0 ft, q = 1.89 x 10^{-5} ft/s. This graph represents baseflow conditions.

The bottom of the well appears to become completely isolated from the diurnal stream temperature fluctuations as is estimated in the calculated values. The clear departures in the theoretical ground water temperature represent a discrete flow path that would be capable of enhancing or reducing the thermal gradient.

Again we find a fairly uniform flux into the subsurface at shallow depths, and thus stream stage playing a minor role in the subsurface response characteristics. As noted earlier the analytical predictions take into account the temperature dependant flux. Together these suggest that for the observation period the stream water characteristics within the reach impact the ground water dynamics only at a shallow depth.

The adaptation of the heat flow equation (Equation 2) to this study proved very useful and helped to confirm some suggested interactions. The strengths of the model are its ease of use, flexibility and the self-correcting nature regarding the initial boundary conditions. As pointed out earlier, it fails to account for additional heat sources and/or sinks, such as a deeper ground water flow path. The results of the predicted ground water temperatures also require, if values are not measured, an estimation of the thermal conductivity, density, specific heat capacity and porosity of the porous medium. This adaptation would likely be useful for unsaturated sediments, but care should be given to use of a well versus a buried temperature probe.

Conceptual Flow Net

From the thermal data, it is possible to derive this conceptual flow net (Figure 35) of the subsurface, adding a 3rd dimension, depth, to the overall ground water exchange. The vertical Darcy velocity is over 300 times greater than the horizontal velocity and thus the flux appears almost vertical in the shallower depths.

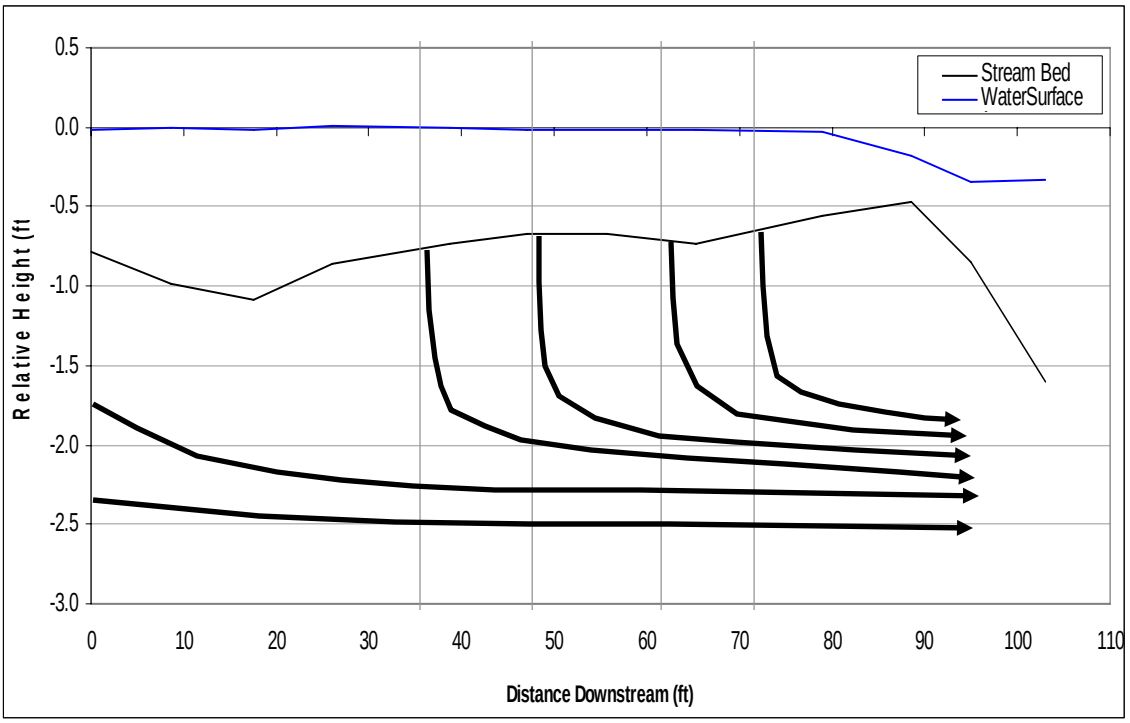

Figure 35. Conceptual Flow Net from Thermal Data (note that vertical scale is exaggerated.)

It is unclear how much contribution variances in depth of the flow paths produce advective response in the ground water temperature.

Hydraulic and Thermal Exchange Rates

From the thermal results and the hydraulic results we obtain a difference in the estimated loss from the stream to the ground water. The loss over the surface of the stream bed is calculated using Equation 4

$$Q = w*l*q \qquad \text{Equation 4}$$

Where Q is the discharge as a volume of water over a discrete time step from the stream to the subsurface, w is the width of the stream at bankfull and average base flow, and l is the length of the reach. The Darcy velocity (q) in the hydraulic-based estimation is calculated from the average hydraulic gradient between the stream and the instream wells

and the hydraulic conductivity measured in the slug tests. The thermal-based flux was the best fit value from the analytical solution at a shallow depth. The results of the two estimations are presented in Table 6.

Hydraulic gradient-based flux		Temperature-based Flux	
Q_{bkf}	Q_{base}	Q_{bkf}	Q_{base}
0.43	0.21	0.40	0.20

Table 6. Estimated discharge (cfs) in the reach using hydraulic gradient-based flux and temperature-based flux. Q_{bkf} is the discharge at bankfull flow and Q_{base} is the discharge at the average baseflow.

The difference represents approximately a 28% reduction in the Darcy velocity from the hydraulic gradient data to the temperature data. The consistency of the estimated ground water temperature to the measured data represents a better estimate over time than the hydraulic-based data and at a large cost savings to hydraulic-based continuous data. To highlight this, a researcher or restoration practitioner could instrument 7 wells with 3 temperature data loggers for about the same price of 1 pressure transducer.

Predicted Change in Exchange

The structure proposed at the study site is a “baffle” constructed of native materials. The structure is a right triangle running 24 ft along the left bank and at the downstream side it sticks out 13 ft into the stream channel (Figure 35).

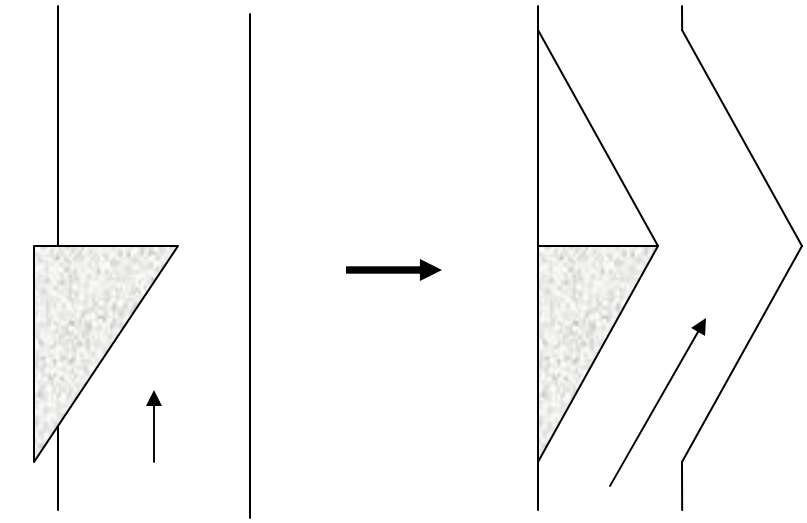

Figure 36. Conceptual drawing of proposed channel-modifying structure.

The purpose of the structure is to slow the water velocity through the structure allowing entrained sediments to deposit and create a point bar while redirecting swifter water around the structure forming a new thalwag. The downstream side of the structure will also exhibit slow velocities and thus the point bar grows by twice the structure size. The length of the channel is expected to grow by at least the hypotenuse of the structure plus an equal length on the downstream side. The overall length of the reach increases from 48 ft to 55 ft.

Adding stream length with the proposed structure increases the total estimated exchange to 0.49 cfs at bankfull and 0.24 cfs at baseflow based on the hydraulic gradient based estimation and approximately 0.45 cfs at bankfull and 0.23 cfs at baseflow using thermal-based estimation. This flow is not expected to produce a net loss for the stream. Instead this refers to an increase in residence time of water in the subsurface.

V. Conclusions

The data presented here were collected from the Rio de las Vacas study site over 13 months in 2007 and 2008. The description of the reach and its ground water / surface water interactions present a complex system where temperature plays an important role. It was determined that the reach is a losing stream at shallow depths, with parallel ground water flow at depth and in the stream banks. The laminar ground water flow is considerably more stable in temperature and is generally cooler with depth in spring, summer and fall months (warmer in the winter months). The contribution to the subsurface flow at depth in the study reach is determined by upstream dynamics and the contribution of stream flow within the reach to the subsurface is found to be limited. As ground water temperature dynamics are not correlated with the stream stage in time, the disruption in classic subsurface temperature profiles may be dictated by upstream infiltration that on a diurnal time step is temperature dependant or the result of a conductive heat transfer with deeper ground water. The temperature-based exchange estimations provide a slightly different discharge value of stream water to the subsurface than the hydraulic-based exchange estimation. This study has confirmed the use of temperature data loggers as a low cost, robust alternative for monitoring directional changes and magnitude of this exchange over small time steps. The predicted gains in stream loss to the subsurface are between 0.05 to 0.06 cfs for an estimated 7 feet of added stream length from the proposed structure. The minimal gains in the exchange, would likely not counter the increase in stream temperatures from increased exposure to solar radiation. Therefore additional measures, such as planting woody vegetation for shade, are required to offset overall increases in stream temperatures.

References

Anderson, M. P. 2005. Heat as a Ground Water Tracer. *Ground Water*, Vol. 43, No. 6, pp. 951-968.

Baxter, C. V. and F. R. Hauer. 2000. Geomorphology, hyporheic exchange and selection of spawning habitat by bull trout (*Salvelinus confluentus*). *Canadian Journal of Fisheries and Aquatic Sciences* 57: 1470-1481.

Baxter, C., and R. F. Hauer. 2003. Measuring groundwater-stream water exchange: New techniques for installing minipiezometers and estimating hydraulic conductivity. *Transactions of the American Fisheries Society* 132: 493-502.

Benson, N. G. 1953. The importance of groundwater to trout populations in the Pigeon River, Michigan. Proceedings of the North American Wildlife Conference 18: 269-281.

Boulton, A. J., H. M. Valett, and S. G. Fisher. 1992. Spatial distribution and taxonomic composition of the hyporheos of several Sonoran desert streams. *Archiv für Hydrobiologie* 125, no.1: 37-61.

Bouwer, H. and R. C. Rice. 1976. A Slug test for determining hydraulic conductivity of unconfined aquifers with completely or partially penetrating wells. *Water Resouces Research* 12: 423-428.

Coleman, R. J. and C. N. Dahm. 1990. Stream geomorphology: effects on periphyton standing crop and primary production. *Journal of the North American Benthological Society* 9: 293-302.

Coleman, M. J. and H. B. N. Hynes. 1970. The vertical distribution of invertebrate fauna in the bed of a stream. *Limnology and Oceanography* 15: 31-40.

Constantz, J., Thomas, C. L., and Zellweger, G. 1994. Influence of diurnal variations in stream temperature on streamflow loss and groundwater recharge. *Water Resources Research*. 30: 3253-3264.

Cunjak, R. A. and G. Power. 1986. Winter habitat utilization by stream resident brook trout (*Salvelinus fontinalis*) and brown trout (*Salmo trutta*). *Canadian Journal of Fisheries and Aquatic Sciences* 43: 1970-1981.

Curry, R. A. and D. L. G. Noakes. 1995. Groundwater and the selection of spawning sites by brook trout, *Salvelinus fontinalis*. *Canadian Journal of Fisheries and Aquatic Sciences* 52: 1733-1740.

Dahm, C. N., D. L. Carr, and R. L. Coleman. 1991. Anaerobic carbon cycling in stream ecosystems. *Verhandlungen der Internationalen Vereinigung für theoretische und angewandte Limnologie* 24: 1600-1604.

Dahm, C. N., N. B. Grimm, P. Marmonier, H. M. Valett, and P. Vervier. 1998. Nutrient dynamics at the interface between surface waters and groundwaters. *Freshwater Biology* 40: 427-451.

Dahm, C. N. and H. M. Valett. 1996. Hyporheic zones. Pages 107-119 in F. R. Hauer and F. A. Lamberti editors. Methods I Stream Ecology. Academic Press, San Diego, California.

Danielopol, D. L. 1989. Groundwater fauna associated with riverine aquifers. *Journal of the North American Benthological Society*. 8: 18-35.

Deming, David. 2002. Introduction to Hydrogeology. McGraw-Hill Higher Education. New York, NY.

Duff, J. H. and F. J. Triska. 1990. Denitrification in sediments from the hyporheic zone adjacent to a small forested stream. *Canadian Journal of Fisheries and Aquatic Sciences*. 47: 1140-1147.

Ebersole, J. L., W. J. Liss, and C. A. Frissell. 2001. Relationship between stream temperature, thermal refugia and rainbow trout *Oncorhynchus mykiss* abundance in arid-land streams in the northwestern United States. *Ecology of Freshwater Fish.* 10: 1-10.

Ferrell, S., S. Eddy, D. Goodman, K. Lund, and J Simino. 2003. Rio de Las Vacas: Stream inventory report, Santa Fe National Forest, http://www.fs.fed.us/r3/sfe/fish/reports/stream_inventory_reports/index.html

Fortner, S. L. and D. S. White. 1988. Interstitial water patterns: a factor influencing the distribution of lotic aquatic vascular macrophytes. *Aquatic Botany* 31: 1-12.

Garrett, J. W., D. H. Bennett, F. O. Frost, and R. F. Thurow. 1998. Enhanced incubation success for Kokanee spawning in groundwater upwelling sites in a small Idaho stream. *North American Journal of Fisheries Management* 18: 925-930.

Geist, D. R., M. C. Joy, D. R. Lee, and T. Gonser. 1998. A method for installing piezometers in large cobble beddrivers. *Ground Water Monitoring and Remediation*. 18: 78-82.

Giller, P. S. 2005. River restoration: Seeking ecological standards. Editor's introduction. *Journal of Applied Ecology* 42: 201-207.

Grimm, N. B., and S. G. Fisher. 1984. Exchange between interstitial and surface water: implications for stream metabolism and nutrient cycling. *Hydrobiologia* 111: 219-228.

Halford, K. J. and Kuniansky, E. L. 2002. Spreadsheets for the Analysis of Aquifer-Test and Slug-Test Data, Version 1.2, Open File Report 02-197.

Hansen, E. A. 1975. Some effects of groundwater on brown trout. *Transactions of American Fisheries Society* 104, no. 1: 100-110.

Harvey, J. W., and K. E. Bencala. 1993. The effect of streambed topography on surface-subsurface water exchange in mountain catchments. *Water Resource Research* 29, no. 1: 89-98.

Hill, A. R. 1990. Groundwater flow paths in relation to nitrogen chemistry in the near-stream zone. *Hydrobiologia* 206: 39-52.

Hemond, H. F. 1990. Wetlands as the source of dissolved organic carbon to surface waters. Pages 301-313 in E. M. Perdue and E. T. Gjessing, eds., Organic Acids in Aquatic Ecosystems, John Wiley and Sons, Ltd.

Hendricks, S. P. 1993 Microbial ecology of the hyporheic zone: A perspective integrating hydrology and biology. *Journal of the North American Benthological Society* 12: no. 1: 70-78.

Hendricks, S. P. and D. S. White. 1988. Hummocking in lotic *Chara*: Observations on alterations of hyporheic temperature patterns. *Aquatic Botany* 31: 13-22.

Henry, K.S., H. M. Valett, J.A. Morrice, C. N. Dahm, G. J. Wroblicky, M.A. Santistevan, and M. E. Campana. 1994. Ground water – surface water exchange in two headwater streams. *Proceedings of the Second International Conference on Ground Water Ecology* (eds J. A. Stanford & H. M. Valett), pp. 319-328. American Water Resources Association, Herndon.

Jenkins, M. 2003. Prospects for biodiversity. *Science* 302:1175-1177.

Jobson, H. E., and W. P. Carey. 1989. Interaction of fine sediment with alluvial streambeds. *Water Resources Research*. 25, no. 1: 135-140.

Keys, W. S. and R. F. Brown. 1978. The use of temperature logs to trace the movement of injected water. Ground Water 16, no. 1: 32-48.

Kondolf, G. M., J. W. Webb, M. J. Sale and T. Felando. 1987. Basic hydrologic studies for assessing impacts of flow diversions on riparian vegetation: examples from streams of the eastern Sierra Nevada, California, USA. *Environmental Management*.11: 757-769.

Lee, D. R. and H. B. N. Hynes. 1977. Identification of groundwater discharge zones in a reach of Hillman Creek in southern Ontario. *Water Pollution Research in Canada* 13: 121-133.

Lowrance, R., R. Todd, J. Fail, O. Hendrickson, R. Leonard, and L. Asmussen. 1984. Riparian forests as nutrient filters in agricultural wetlands. *BioScience* 34: 374-377.

New Mexico Water Quality Commission (NMWQC), "2004-2006 State of New Mexico Integrated Clean Water Act §303(d) §305(b) Report", http://www.nmenv.state.nm.us/wqcc/303d-305b/2004/index.html

New Mexico Water Quality Commission (NMWQC), "Water Quality and Water Pollution Control in New Mexico ~ 1998", http://www.nmenv.state.nm.us/swqb/305b/1998/305b_98.html

Nielsen, J. L., T. E. Lisle, and V. Ozaki. 1994. Thermally stratified pools and their use by steelhead in northern California streams. *Transactions of the American Fisheries Society*. 123: 613-626.

Palmer, M. A., E. S. Bernhardt, J. D. Allan, P. S. Lake, G. Alexander, S. Brooks, J. Carr, S. Clayton, C. N. Dahm, J. Follstad Shah, D. L. Galat, S. G. Loss, P. Goodwin, D. D. Hart, B. Hassett, R. Jenkinson, G. M. Kondolf, R. Lave, J. L. Meyer, T. K. O'Donnell, L. Pagano, and E. Sudduth. 2005. Standards for ecologically successful river restoration. *Journal of Applied Ecology* 42: 208-217.

Peterjohn, W. T. and D. L. Correll. 1984. Nutrient dynamics in an agricultural watershed: observations on the role of a riparian forest. *Ecology* 65: 1466-1475.

Riggs, H. C. 1985, Streamflow characteristics. Elsevier, New York.

Savant, S. A., D. D. Reible, and L. J. Thibodeaux. 1987. Convective transport within stable river sediments. *Water Resources Researc*h 23, no. 9:1763-1768.

Schwartz, F. W. and H. Zhang. 2003. Fundamentals of Ground Water. John Wiley and Sons, Inc. New York, NY.

Silliman, S. E., and D. F. Booth. 1993. Analysis of time-series measurements of sediment temperature for identification of gaining vs. losing portions of Juday Creek, Indiana. *Journal of Hydrology* 146: 131-148.

Silliman, S. E., J. Ramirez, and R. L. McCabe. 1995. Quantifying downflow through creek sediments using temperature time series: One-dimensional solution incorporating measured surface temperatures. *Journal of Hydrology* 167: 99-119.

Sowden, T. K. and F. Power. 1985. Prediction of rainbow trout embryo survival in relation to groundwater seepage and particle size of spawning substrates. *Transactions of the American Fisheries Society* 114: 804-812.

Stanford, J. A., J. V. Ward and B. K. Ellis. 1994. Ecology of the alluvial aquifers of the Flathead River Montana. Pages 367-389 in J. Gilbert, D. L. Danielopol and J. A. Sanford, editors. Groundwater ecology. Academic Press, San Diego, California.

Stonestrom, D. A. and J. Constantz. 2003. Heat as a Tool for Studying the Movement of Ground Water Near Streams. United States Geological Survey Circular 1260.

Torgersen, C. E., R. N. Faux, B. A. McIntosh, N. J. Poage and D. J. Norton. 2001. Airborne thermal remote sensing for water temperature assessment in rivers and streams. *Remote Sensing of Environment*. 76: 386-398.

Triska, F. J., V. C. Kennedy, R. J. Avanzino, G. W. Zellweger, and K. E. Bencala. 1989. Retention and transport of nutrients in a third-order stream in northwestern California: hyporheic processes. *Ecology* 70: 1893-1905.

Triska, F. J., V. C. Kennedy, R. J. Avanzino, G. W. Zellweger, and K. E. Bencala. 1990. In situ retention-transport response to nitrate loading and storm discharge in a third-order stream. *Journal of the North American Benthological Society* 9: 229-239.

Triska, F. J., J. H. Duff, and R. J. Avanzino. 1993. Patterns of hydrologic exchange and nutrient transformation in the hyporheic zone of a gravel-bottom stream: Examining terrestrial-aquatic linkages. *Freshwater Biology* 29: 259-274.

Valett, H. M. 1993. Surface-hyporheic interactions in a Sonoran desert stream: Hydrologic exchange and diel periodicity. *Hydrobiologia* 259:133-144.

Valett, H. M., C. C. Hakenkamp, and A. J. Boulton. 1993. Perspectives on the hyporheic zone: integrating hydrology and biology. Introduction. *Journal of the North American Benthological Society* 12: 40-43.

Vaux, W. G. 1962. Interchange of stream and intergravel water in a salmon spawning riffle. United States Fish and Wildlife Service Scientific Report, Fisheries 405:1-10.

Winter, Thomas C., et al., “Ground Water and Surface Water: A Single Resource, U.S. Geological Survey Circular 1139”, 1998.

Woessner, William H. 2000. Stream and fluvial plain ground water interactions: rescaling hydrogeologic thought. *Ground Water* 38, no. 3: 423-429.

Wolman, M. G. 1954. A method of sampling coarse river-bed material. Transactions, American Geophysical Union. 35. pp. 951-956.

Woods, P.F. 1980. Dissolved oxygen in intergravel water of three tributaries to Redwood Creek, Humboldt County, California. *Water Resources Bulletin,* AWRA 16, no.1. 105-111.

Wroblicky, G. J., M. E. Campana, H. M. Valett, J. A. Morrice, K. S. Henry, C. N. Dahm, J. V. Hurley and J. M. Noe. 1992. Remote monitoring of stream hyporheic zones with inexpensive pressure transducer-data acquisition systems, proceedings of the first international conference on ground water ecology (eds. J. A. Stanford and J. J. Simons), pp 267-277, American Water Resources Association, Bethesda.